

Cloud classifications with the SCANDIA model

Karl-Göran Karlsson

Cloud classifications with the SCANDIA model

Karl-Göran Karlsson

*Cover: Example of SCANDIA cloud classification for the northern European area
from 8 April 1995 at 11:54 UTC*

Report Summary / Rapportsammanfattning

Issuing Agency/Utgivare		Report number/Publikation	
Swedish Meteorological and Hydrological Institute S-601 76 NORRKÖPING Sweden		RMK No. 67	
		Report date/Utgivningsdatum	
		January 1996	
Author (s)/Författare			
Karl-Göran Karlsson			
Title (and Subtitle/Titel			
Cloud classifications with the SCANDIA model.			
Abstract/Sammandrag			
<p>The cloud classification model SCANDIA (SMHI Cloud ANalysis model using DIgital AVHRR data) is described in this report. SCANDIA is based on multispectral processing of NOAA AVHRR imagery where cloud and surface analyses are produced in real-time for use in operational weather forecasting. Also other applications are described, e.g. compilation of cloud climatologies, estimation of snow area coverage and validation of cloud forecasts from numerical weather prediction models.</p> <p>Two different versions of the SCANDIA model are discussed. The first version was introduced in 1988 and the model structure is explained in detail. Model strengths and weaknesses are described by using comparisons with observed cloudiness from ordinary surface weather observations (SYNOP). Also the feedback response from operational weather forecasters is discussed. The second version was introduced in 1994, now operating on a larger area covering the major parts of northern Europe. Necessary modifications for operating on larger scales are described and new features for the identification and highlighting of situations with serious limitations of classification results are demonstrated.</p>			
Key words/sök-, nyckelord			
Cloud classification, AVHRR, multispectral processing, cloud climatologies, validation of cloud forecasts, class separabilities			
Supplementary notes/Tillägg		Number of pages/Antal sidor	Language/Språk
		36	English
ISSN and title/ISSN och titel			
0347-2116 SMHI Reports Meteorology Climatology			
Report available from/Rapporten kan köpas från:			
SMHI S-601 76 NORRKÖPING Sweden			

1. INTRODUCTION

The amount of image information from weather satellites is high today and it will increase substantially in the near future with the introduction of new sensors on coming satellites (e.g. the AVHRR/3 sensor on the NOAA satellites and the SEVIRI instrument on the MSG satellites - see acronym list at the end of the report). Since the time to spend on manual image interpretation is very limited in the operational environment of a modern weather service (especially in Nowcasting applications), automatic image interpretation techniques and special image enhancing methods are growing in importance. One of the most obvious methods here is the use of image classification.

The basic idea of image classification is to extract specific information about various objects or surfaces in satellite imagery and present it in a form that is more user friendly and useful. In this way, the interpretation of satellite imagery may be facilitated (e.g. for monitoring cloudiness and precipitation conditions in operational weather forecasting). Another prominent reason for classification is further to accomplish a reduction in data volume although retaining the most important information, alternatively increasing the value of the information. This reduction in data volume would then enable distribution of the data to a large number of external users. A third and quite important reason is to enable a quantitative use of satellite imagery, e.g. for climate investigations. Since data volumes from future satellites will increase considerably compared with today, image classification and other processing methods are foreseen to increase in importance in the future.

Many automatic and objective cloud and surface analysis schemes using satellite imagery have been developed throughout the years. Both single-channel and multispectral data has been used. The most interesting and promising methods using weather satellite imagery have been based on data from the NOAA AVHRR instrument. Here, the very different spectral characteristics in the VIS, the mixed VIS-IR and the IR spectral regions may be utilised to produce quite advanced cloud and surface analyses. Several schemes have been described, e.g. by Coakley and Bretherton, 1982, Eyre *et al*, 1984, d'Entremont, 1986 and Inoue, 1987. However, this report deals only with schemes that have become available as operational tools in weather forecasting based on operationally available satellite imagery over the European area.

The most firmly established and used operational schemes in Europe which are based on AVHRR data are the following: the APOLLO scheme (Saunders and Kriebel, 1988), the SCANDIA model (Karlsson and Liljas, 1990 and Karlsson, 1995) and the CMS Lannion cloud masking scheme (Derrien *et al*, 1993). Other operational schemes have also been introduced in recent years (e.g. Dybbroe, 1995). All these schemes are very similar in their main principles in trying to separate clouds and surface classes through the use of their different and typical spectral signatures. A common feature of all these schemes are that they are all multispectral thresholding schemes. Thresholds have been determined subjectively from empirical studies (in so-called *supervised training and classification* sessions) or through the use of radiative transfer models. Unsupervised methods with more objective decision rules (often called *clustering methods*) are not that frequently used but several schemes have been tested and proposed (e.g. by Raustein, 1989 and Desbois *et al*, 1982).

A quite thorough and detailed description of the SCANDIA model will be given in this report. This model has been operated for several years and considerable experience with

the multispectral classification technique has been gained. The model structure, different applications and quality characteristics will be discussed. Applications outside the traditional use as a tool in operational forecasting (e.g. cloud climate investigations) are also presented.

2. HISTORY OF THE SCANDIA MODEL

The idea of an operational cloud analysis scheme, based on digital AVHRR data, was proposed at SMHI in the early 1980s (Liljas, 1982 and 1984). Several years of spectral signature studies followed where different cloud and surface types were examined. Typical reflectivity, transmissivity and emissivity characteristics were monitored for each cloud and surface type depending on varying solar elevations, airmass changes and different AVHRR sensors (AVHRR/1 with four channels and AVHRR/2 with five channels). The use of the 3.7 μm channel was found particularly important and promising (see Liljas, 1986). After defining the main principles for an operational cloud classification method (Karlsson, 1989), the final classification scheme, named SCANDIA (the SMHI Cloud Analysis model using Digital AVHRR data), was implemented in 1988. This version of the SCANDIA model was described in detail by Karlsson and Liljas (1990). An upgraded version of the model was later introduced in 1994 for execution on larger geographical scales. Both the original and the upgraded versions are discussed below.

3. STRUCTURE OF THE ORIGINAL SCANDIA MODEL

The classification model makes use of calibrated and geometrically transformed imagery from all five AVHRR channels at maximum horizontal resolution (at nadir 1.1 km). AVHRR scenes are classified by using seven image features which are listed in Table 1. Classifications are made in two pre-defined areas, covering the northern and southern parts of the Nordic area. Each pixel in a scene is classified into one of 23 cloud and surface types (see Table 2). The main use of each classification feature is summarised in Table 1. Feature 4 is here central for the classifier. This feature is based on AVHRR channel 3 brightness temperatures related to brightness temperatures in AVHRR channel 4 forming a brightness temperature difference. The feature plays a major role in the cloud/no-cloud discrimination, for both day and night. The strength of the feature is to enable discrimination of clouds and snow surfaces during day and to map low and mid-level water clouds during night despite small temperature differences between the surface and the cloud tops.

SCANDIA is a supervised thresholding model, where typical class domains are defined by hyperboxes in a seven-dimensional feature space. In principle, a classical box model is used but several threshold tests (outer limits) have been omitted for optimisational reasons. On the other hand, each class is often described by several boxes in order to compensate for elongated or skewed pixel distributions in feature space.

A unique set of thresholds is defined for each of several pre-defined categories related to existing illumination conditions, weather types and satellites. The season (one of the set "Summer, Spring, Winter, Autumn" - defined in Table 3), the current sun elevation (determined by one of 12 sun elevation intervals - defined in Table 4) and the satellite number specify which category and thus which set of thresholds that is used to classify the scene in each of the two areas.

In total, 96 different categories are necessary to adapt the cloud classification model to the seasonal and daily changes in classification conditions. A more direct dependence on the current weather situation is furthermore included by using temperature information at the 700 hPa and 500 hPa levels. This information is taken from meteorological objective analyses and is used for threshold tests in feature 5 (see Table 1). The purpose of using this temperature information is to achieve a more dynamic adaptation of decision borders for the separation of the main cloud groups low-, mid- and high-level clouds. The brightness temperatures in feature 5 of thick clouds (here identified as clouds with very low values in feature 6) are compared to the area means of 700 and 500 hPa

Table 1. Classification features used by SCANDIA. Calibrated AVHRR channels are denoted CH1, CH2, CH3, CH4 and CH5. TEX4 means a local (in a 5x5 pixel window) highpass filtering of CH4 followed by a lowpass filtering (in an 11x11 pixel window) to measure the small scale variation of brightness temperatures.

Feature number	Composition	Quantity	Main use for classifier
1	CH1	Albedo*	Daytime separation of clouds and snow from land surfaces. Used in combination with feature 4.
2	CH1-CH2	Albedo difference	Daytime separation of land surfaces with vegetation from sea surfaces. Used also for snow detection.
3	Land mask	Land or sea indication	Geographic map used for land/sea-separation at night and for low sun elevations.
4	CH3-CH4	Brightness temperature difference	Separates all clouds from land and sea surfaces during daytime. Important at night for fog, Stratus and Cirrus detection.
5	CH4	Brightness temperature	Separates main cloud groups Low, Medium and High clouds by comparing with mean temperatures at 500 hPa and 700 hPa.
6	CH5-CH4	Brightness temperature difference	Separates thin clouds (especially Cirrus clouds) from thick clouds both night and day.
7	TEX4	Temperature variance	Separates clouds with small scale texture (e.g. Cumulus) from more homogeneous clouds (e.g. Stratus).

*This is not a true albedo. A more correct description is bi-directional reflectance.

temperatures for the separation into the mentioned main cloud groups. This method was found much more realistic during seasonal changes than the use of fixed temperature thresholds.

The 700 and 500 hPa mean temperatures define two threshold parameters denoted T700 and T500. Other parameters are also used to introduce seasonal changes. The most important parameters are listed in Table 5.

A schematic example of the hierarchic model structure for one specific classification category is given in Figure 1. Here A denotes albedo, T denotes brightness temperature and TEX is a texture feature (feature seven in Table 1). The index refers to AVHRR channel. Some of the most important thresholds are shown in the right part of the figure. If

Table 2. Classified cloud types and surface types.

Class description	Class description
Open sea without ice	Cumulus congestus over sea
New ice without snow	Small Cumulonimbus
Snowcover (also on ice)	Extensive Cumulonimbus
Winter forest	Altocumulus and Altostratus
Land (free from snow)	Nimbostratus
Haze or sub-pixel clouds over land	Thin Cirrus over land
Haze or sub-pixel clouds over sea	Thin Cirrus over sea
Fog and Stratus	Cirrus over low level clouds
Stratocumulus	Cirrus over middle level clouds
Small Cumulus over land	Thick Cirrostratus
Small Cumulus over sea	Sunglints
Cumulus congestus over land	

Table 3. Seasons for determination of the seasonal dependence of SCANDIA.

Seasons	Period
Summer	15 May - 15 September
Spring	16 March - 14 May
Winter	15 November - 15 March
Autumn	16 September - 14 November

Table 4. Sun elevation intervals (in degrees).

Sun elevation class	Sun elevation interval (°)
1	< 0.5
2	0.5 - 5.2
3	5.2 - 9.8
4	9.8 - 14.5
5	14.5 - 19.3
6	19.3 - 24.2
7	24.2 - 29.3
8	29.3 - 34.7
9	34.7 - 40.5
10	40.5 - 46.5
11	46.5 - 54.1
12	> 54.1

Table 5. Parameters defining dynamic thresholds for the SCANDIA model. Parameters change values due to seasonal changes or to changes in given weather situations (e.g. T700 and T500).

Parameter	Meaning	Updating
T700	Mean 700 hPa temperature	Continuous
T500	Mean 500 hPa temperature	Continuous
LST	Lowest sea surface temperature	Seasonal
SNOWTEMP	Highest snow surface temperature	Seasonal
ICETEMP	Highest ice surface temperature	Seasonal
WINFOTEMP	Highest winter forest temperature	Seasonal
RISKTEMP	Highest temperature for Cb precipitation	Seasonal
CUMTEXT	Cumulus texture threshold	Seasonal

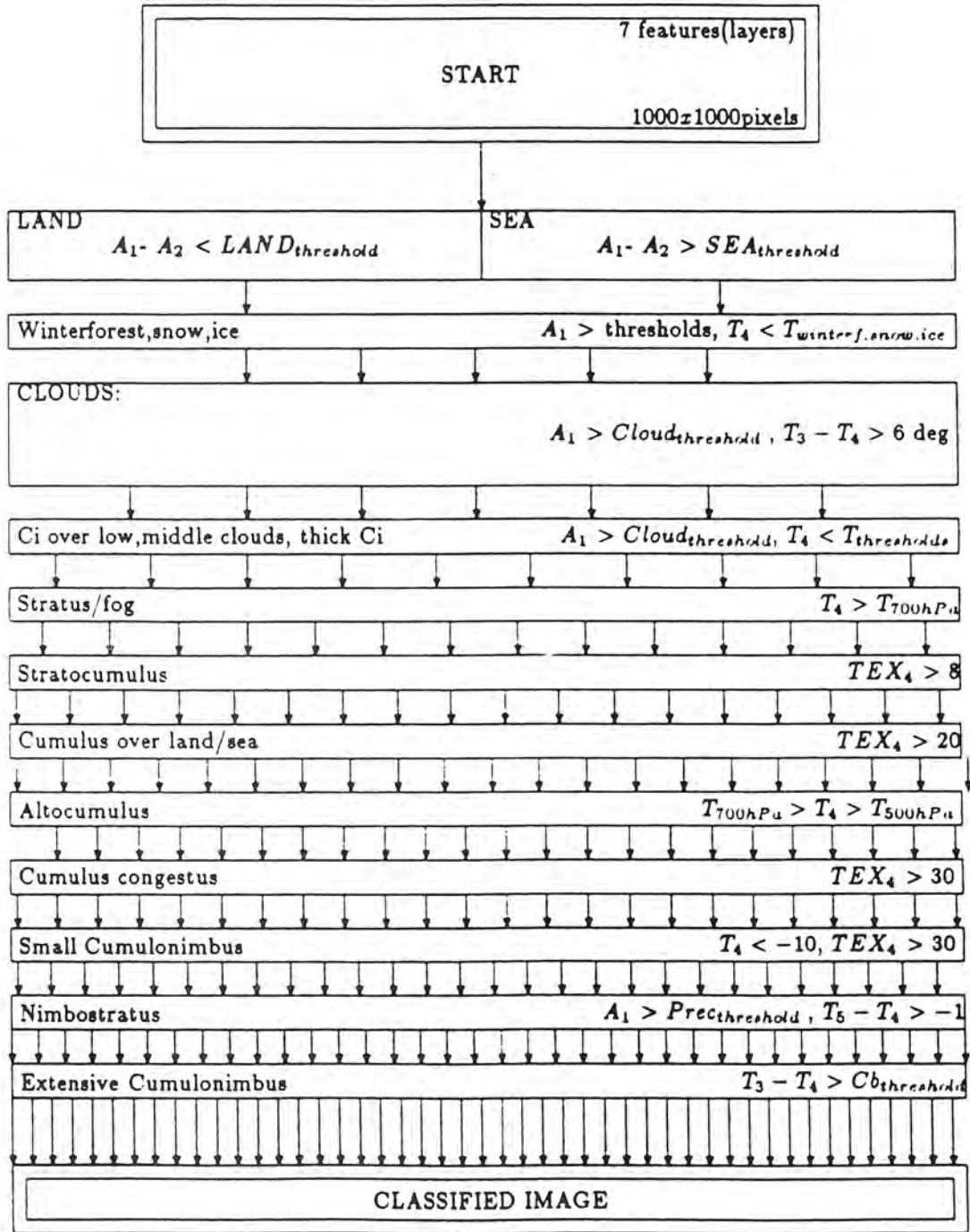


Figure 1. Flow chart exemplifying the hierarchical steps in the classification procedure. Valid during spring at high sun elevations. Important threshold tests are indicated in the right part of the figure. A is albedo and T is brightness temperatures with index numbers denoting AVHRR channel.

the thresholds in a step are matched for the analysed pixel, the labelling is changed to the new class. The increasing number of arrows visualises the separation into an increasing number of classes for each hierarchic step.

Thresholds have been defined by using class mean vectors and covariance matrices from a class database with spectral signatures in the seven-dimensional feature space. This database was defined earlier in the signature study phase. The choice of thresholds was defined subjectively but in a consistent manner, guided by the class database information. The use of a simple thresholding model instead of a more sophisticated statistical model (e.g. a maximum-likelihood classifier) was decided for practical reasons. Operational requirements for accomplishing near realtime execution put hard constraints on cloud classification schemes. Furthermore, it was considered more fruitful to put the main effort into creating a realistic structure for the model (e.g. dependence on sun-elevations, seasons etc.) to enable a dynamic adaptation to the highly variable conditions.

4. KEY CHARACTERISTICS OF THE SCANDIA MODEL

The most significant difference in the SCANDIA model compared with other operational schemes is the use of different sets of thresholds depending on the prevailing sun elevations in a satellite scene. This has been introduced to compensate for apparent anisotropic reflection by clouds and by earth surfaces. Another purpose is that such a formulation is more favourable for realising a fast operational execution since the need for accurate calculations of visible reflectances at pixel resolution (normalisation with the sine of the sun elevation) is avoided. Hence, SCANDIA does thus not use complete calibrated visible bi-directional reflectances but instead original equivalent albedos (use of the nominal calibration coefficients without normalising for the sun elevation).

From Figure 1 we notice that feature 4 together with feature 1 determine the separation of clouds from other objects in an AVHRR scene. During day, brightness temperature differences, as defined by feature 4, are approximating the radiance contribution in AVHRR channel 3 from reflected solar radiation. Clouds reflect substantially in channel 3 as opposed to earth surfaces, with sunglints as a major exception. Although reflection is low from thin ice clouds, a significant temperature difference is also found here due to a higher transmissivity in AVHRR channel 3 than in AVHRR channel 4 for ice clouds. This means that feature 4 alone may be used to define a cloud mask during daytime in the absence of sunglints. Figure 2 shows the SCANDIA threshold in feature 4 for separation of all clouds during daytime, for separation of lower tropospheric water clouds during night and for separation of ice clouds during night. Notice in Figure 2 (and also later in Figure 5) that SCANDIA threshold values are kept constant within each sun elevation interval and are only changed when sun elevation intervals changes (see Table 4).

We notice that during night a negative temperature difference is used for water clouds (because a reflecting object or surface can never radiate as a blackbody). However, to achieve a full cloud separation during night we must account for the fact that thin ice clouds have a positive temperature difference in feature 4 and a negative temperature difference in feature 6 due to the higher transmissivity in the shortest wavelengths in IR. Thick ice clouds and multi-layered clouds are simply handled by using temperature thresholds in feature 5 (parameters T700 and T500 in Table 5). The use of features 4 and 5 at night is visualised in Figure 3.

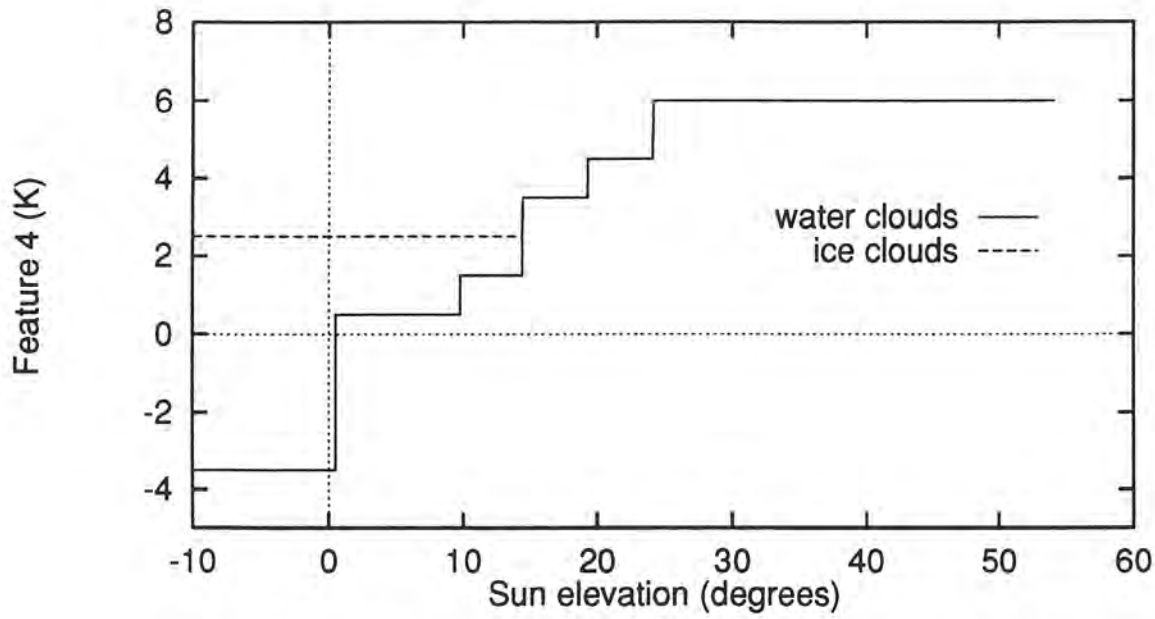


Figure 2. Feature 4 thresholds (temperature differences) as a function of sun elevations for the separation of all clouds from cloud-free surfaces during daytime and for the separation of water and ice clouds from cloud-free surfaces during night.

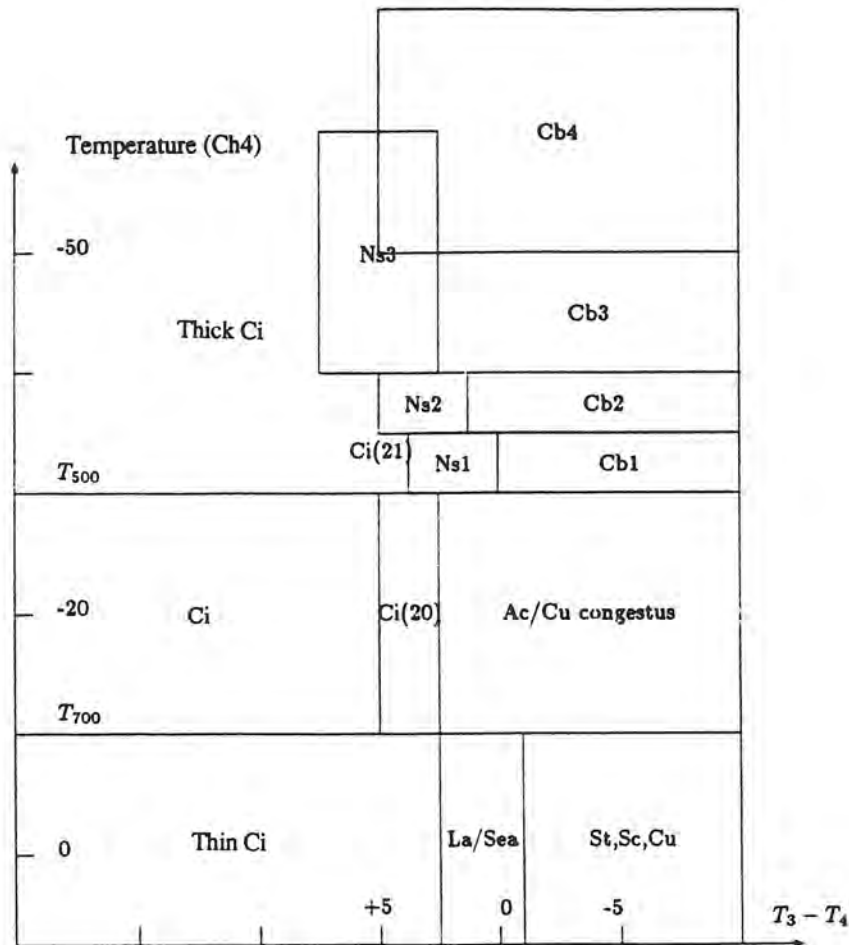


Figure 3. Cloud classification during night using features 4 and 5.

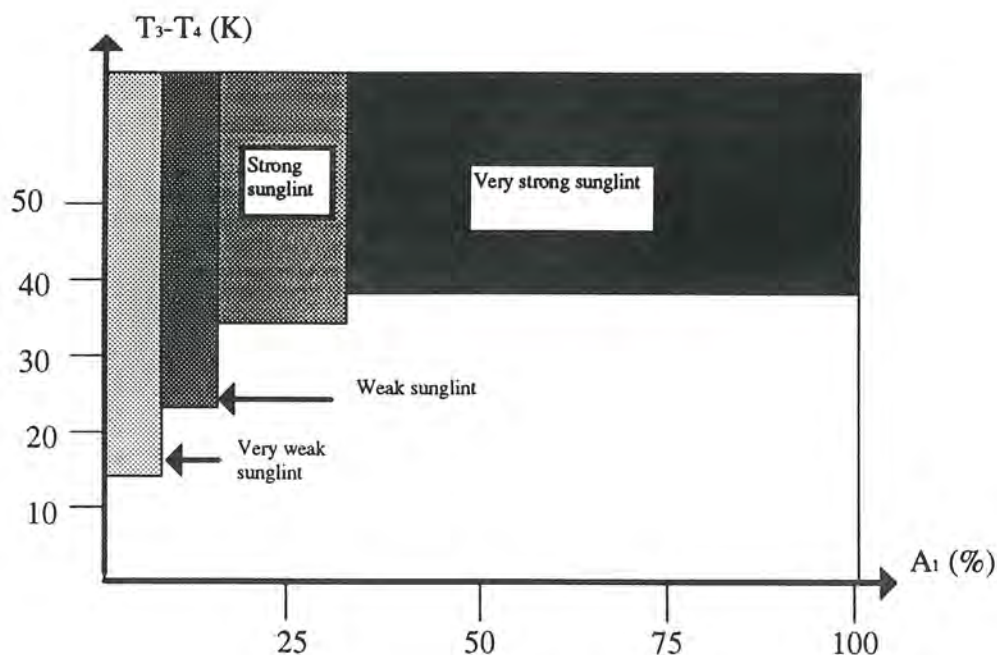


Figure 4. Sunglint discrimination using classification features 1 and 4.

As feature 4 does not permit separation of low-level cloudiness from sunglints during daytime, feature 1 is additionally used here. Sunglints reflect stronger in AVHRR channel 3 than low-level clouds whereas in AVHRR channel 1 conditions are the opposite. The SCANDIA sunglint discrimination method is visualised in Figure 4.

After the basic cloud separation is accomplished, the detailed cloud type separation takes place (compare with Figure 1). Different features are used depending on the cloud type. The anisotropic behaviour of cloud reflection (mainly the increased albedos of clouds at decreasing sun elevations) is treated by using specific thresholds in feature 1. Figure 5 shows the minimum thresholds in each sun elevation interval for Cirrus clouds, Stratocumulus clouds and Nimbostratus clouds as a function of sun elevation. These values represent minimum reflectances as calculated from the constant equivalent albedo threshold at the highest sun elevation in the interval.

A special thresholding application for the three lowest sun elevation intervals is used. Here, both dark situations (at night or if shadows are present) and illuminated conditions are tested for each class at each sun elevation interval. In this way, almost twice as many classes are investigated compared with higher sun elevation intervals.

In addition to cloud type separation, the SCANDIA model also includes qualitative assessments of low-level cloud thickness and likelihood estimations of various precipitation intensity categories. The purpose has been to enhance the value of the cloud classification result in order to facilitate the weather forecaster's analysis of low-level cloud conditions and current precipitation conditions. Different low-level cloud

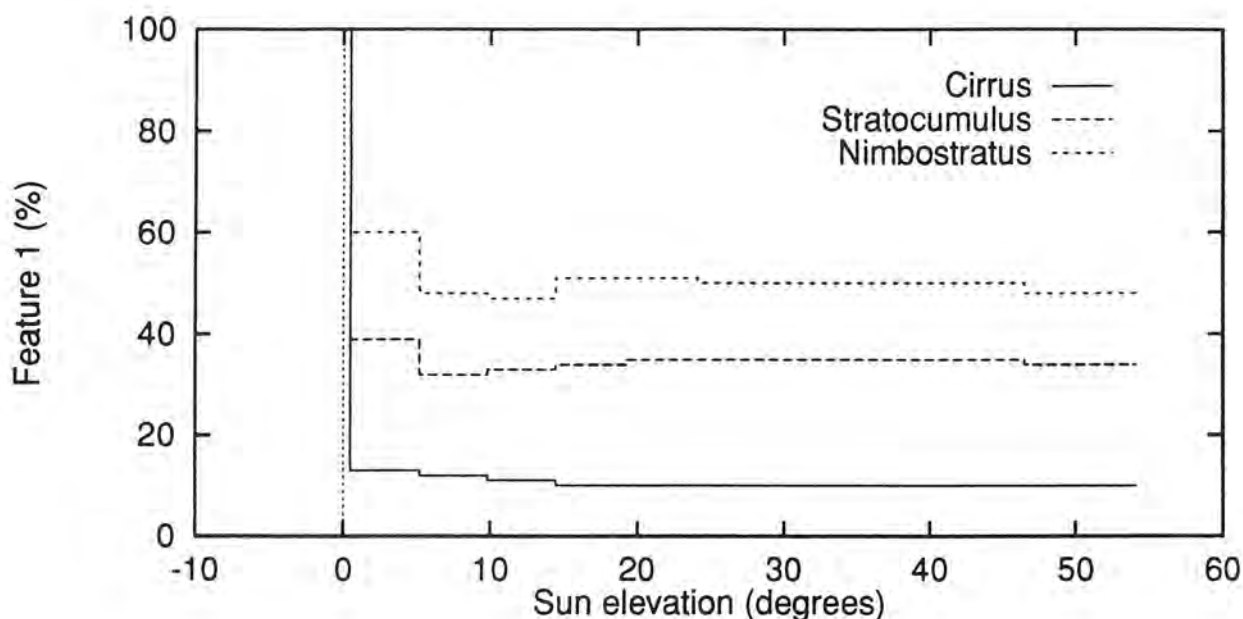


Figure 5. Minimum thresholds in classification feature 1 as a function of sun elevation for thin Cirrus, Stratocumulus and Nimbostratus.

categories (e.g. very thin, thin, medium, thick and very thick) are identified by using feature 4 during night (based on ideas proposed by Eyre et al, 1984) and by use of feature 1 during daytime. Figure 6 shows the night-time separation of low-level cloud types. The daytime scheme is similar but based on different reflectances in AVHRR channel 1. These results must, of course, be used with caution since brightness temperature differences and reflectances vary not only with cloud thickness but also with droplet size and number distributions.

Precipitation analysis is based on the assumption of an existing correlation (however weak) between high precipitation intensities, low feature 5 values and high feature 1 values. Figure 7 shows the basic principles of this precipitation analysis based on these two features. In addition, tests are also performed using features 4 and 6. Feature 4 is used to indicate very active Cumulonimbus clouds with a high probability of heavy precipitation. Such clouds have been found to reflect very strongly in AVHRR channel 3 (as reported by Liljas, 1986 and Setvak and Doswell, 1991). Feature 6 is used to ensure that thin and cold ice clouds are not labelled as precipitating. Since the identification of precipitating clouds in AVHRR imagery is not always obvious or even possible (see Allam *et al*, 1993), an extra category denoted Risk clouds (connected to parameter RISKTEMP in Table 5), defining clouds with a potential of being precipitating, has also been introduced.

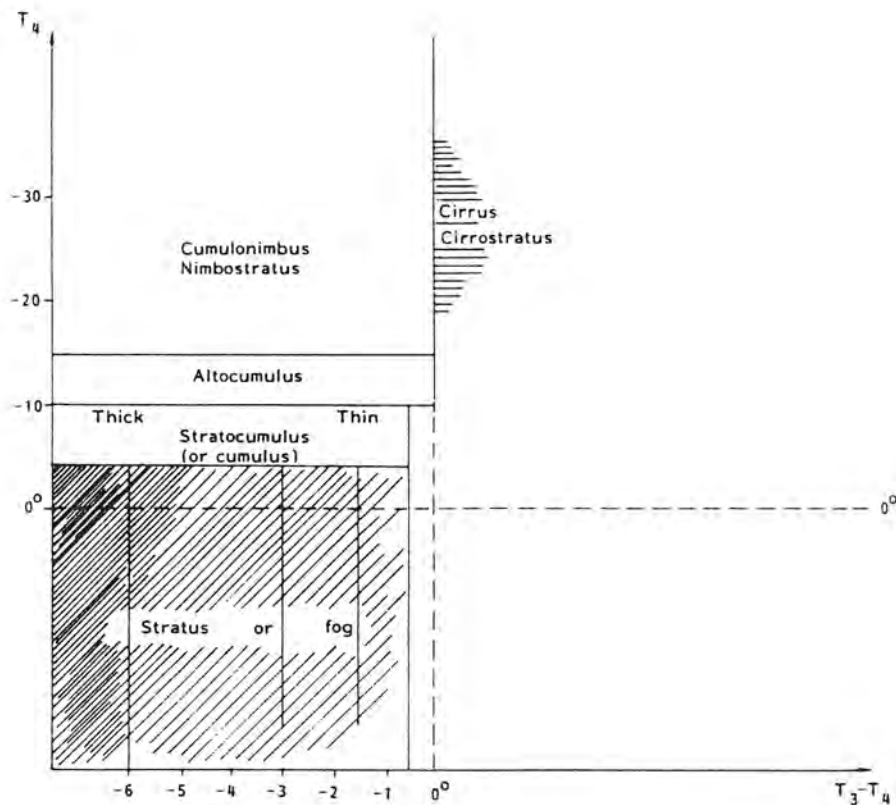


Figure 6. SCANDIA night-time classification of clouds using features 4 and 5. A subdivision of low-level clouds into thickness categories is illustrated with differences in hatching density.

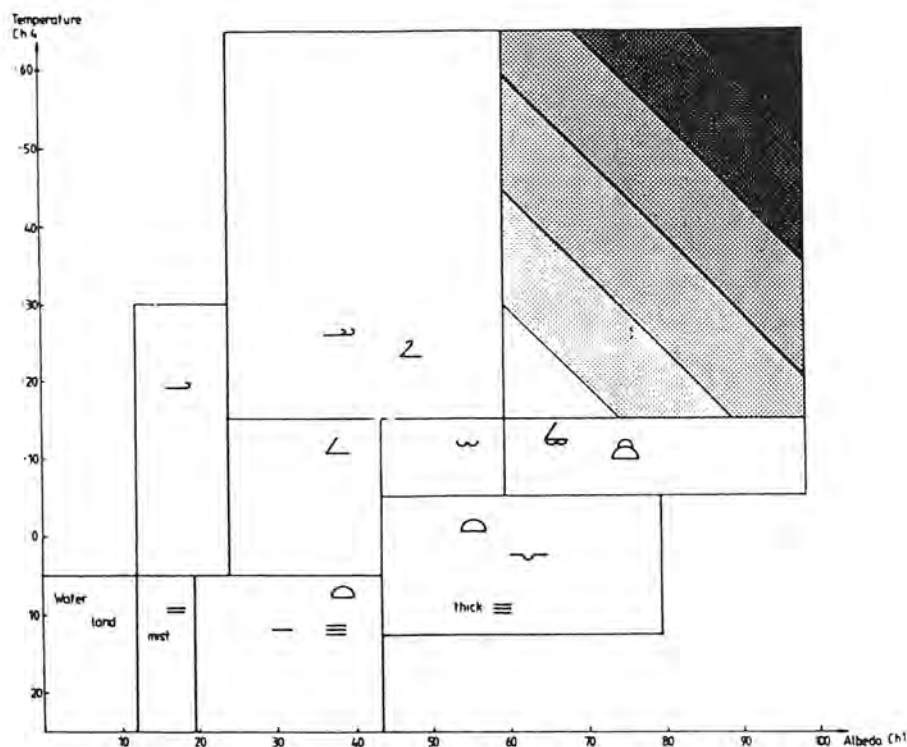


Figure 7. Schematic description of the principles for separation into different precipitation intensity categories. Shaded areas show precipitating clouds and the degree of shading corresponds to different precipitation intensities. A somewhat modified scheme is used in SCANDIA where also other features are used.

5. DEMONSTRATION OF SCANDIA CLOUD CLASSIFICATIONS

Figures 8-12 illustrate the results produced by the SCANDIA model for an AVHRR scene from 25 April 1990 at 12:16 UTC. A frontal cloud system over the Norwegian Sea is approaching Scandinavia. Cumulus convection is occurring over most land areas producing showers. An RGB image (composed by red, green and blue intensity components) with AVHRR channels 1, 2 and 4 over northern Scandinavia is shown in Figure 8 and the SCANDIA cloud classification for the same area is presented in Figure 9. These two figures may be compared to Figure 10 where all classification features (except feature 3 in Table 1) are shown. Notice in particular the importance of feature 4 for the cloud/no-cloud separation, feature 2 for the snow and ice analysis and feature 6 for the analysis of thin clouds.

The presentation of the classification as a precipitation analysis is given in Figure 11. Notice here that non-precipitating clouds are shown in greyshades while precipitating (or potentially precipitating) clouds are shown in yellow and red colours. An example of the presentation of a cloud classification as a qualitative low-level cloud thickness analysis is shown in Figure 12 for a night-time AVHRR scene from 8 October 1991. Low-level clouds are here shown in a colour range from yellow (indicating very thin clouds) to dark red (indicating very thick clouds). Higher cloud types are shown in grey.

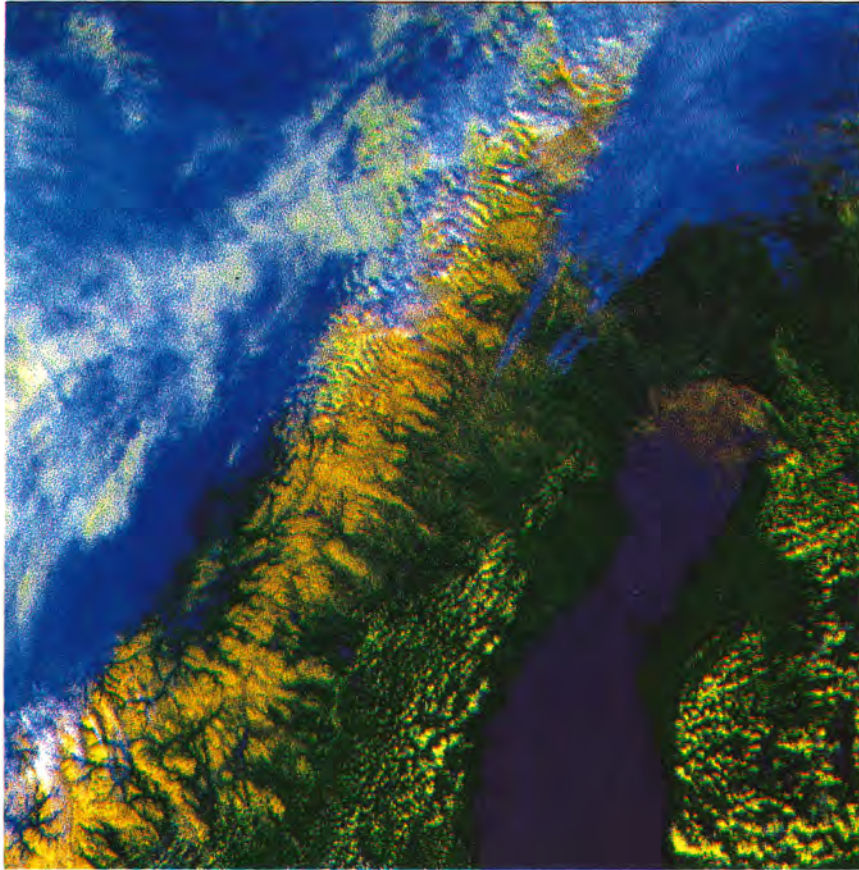


Figure 8. RGB composite image over northern Scandinavia consisting of AVHRR channels 1, 2 and 4 from 25 April 1990 at 12:16 UTC.

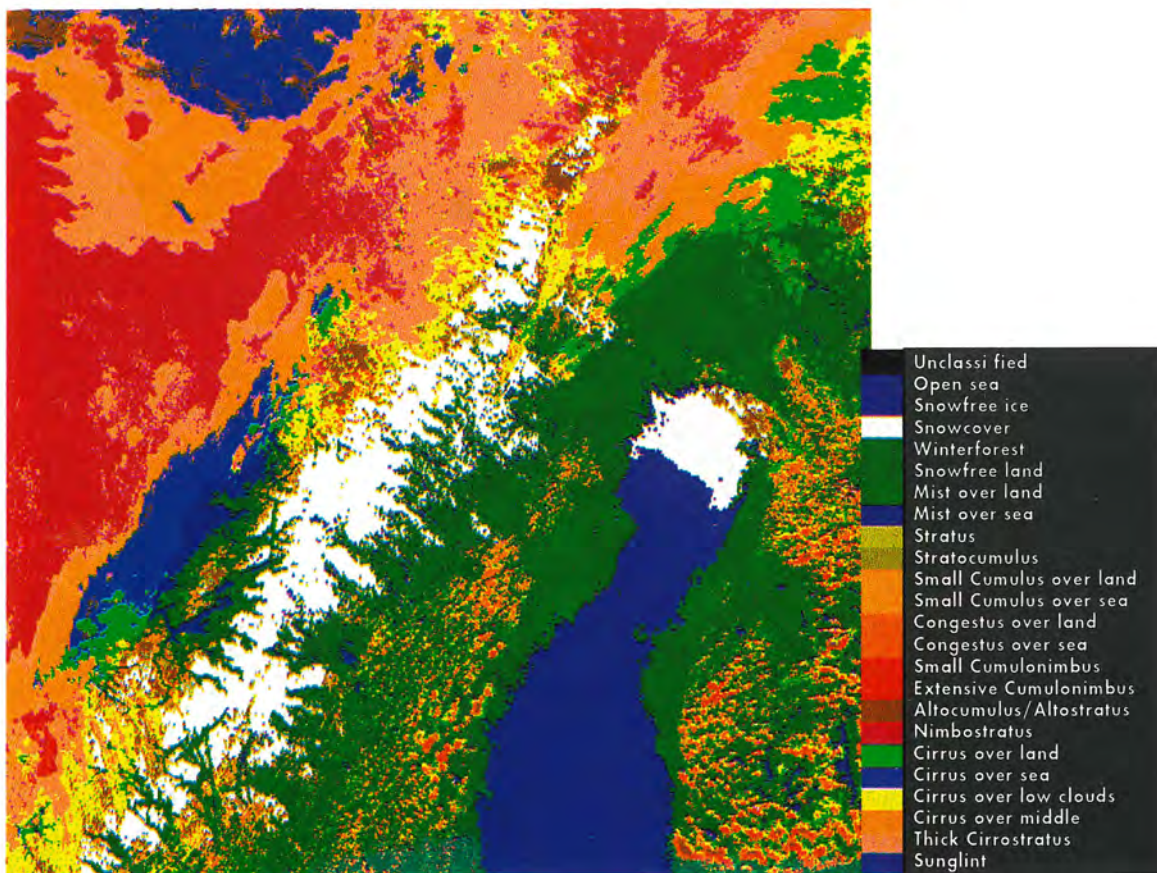
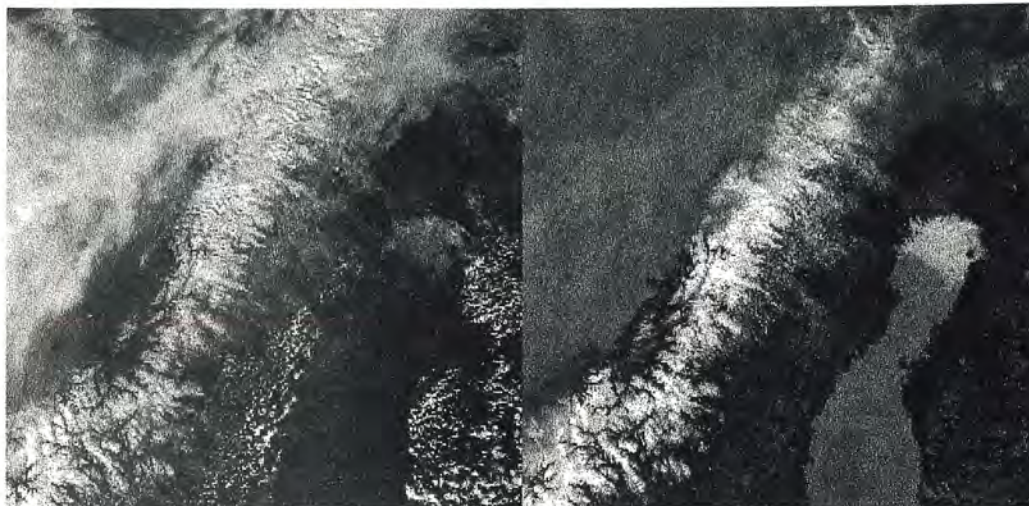
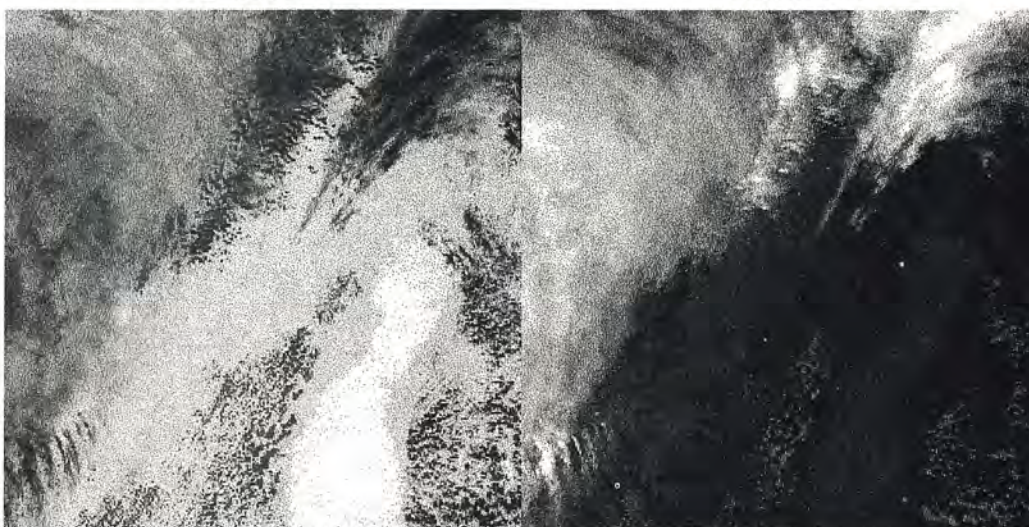


Figure 9. SCANDIA cloud classification for the same AVHRR scene as in Figure 8.



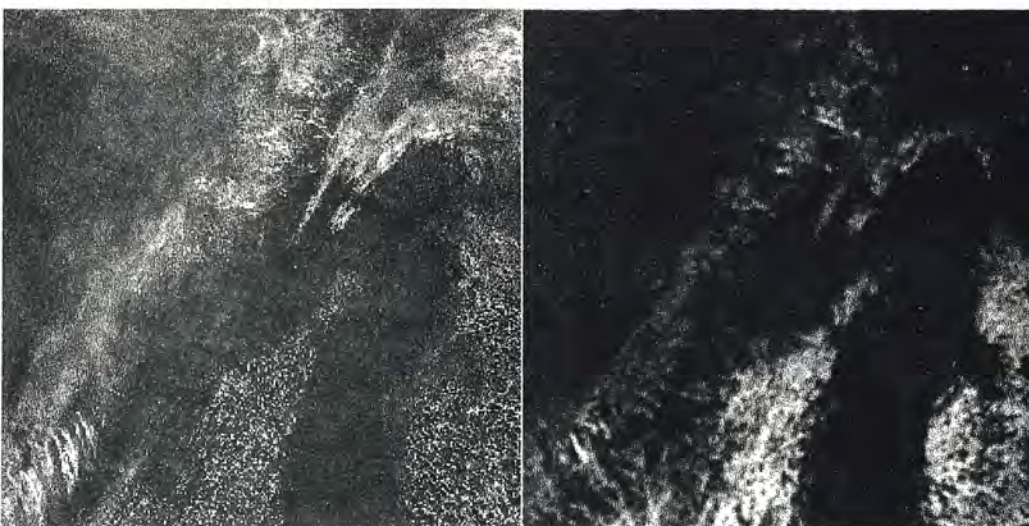
Feature 1

Feature 2



Feature 4

Feature 5



Feature 6

Feature 7

Figure 10 Basic image features for SCANDIA model (compare with Table 1) for the same AVHRR scene as shown in Figures 8 and 9. Contrast stretch operations are applied on all images making positive differences dark (e.g. in features 2 and 4) and negative differences bright (e.g. in features 2 and 6).

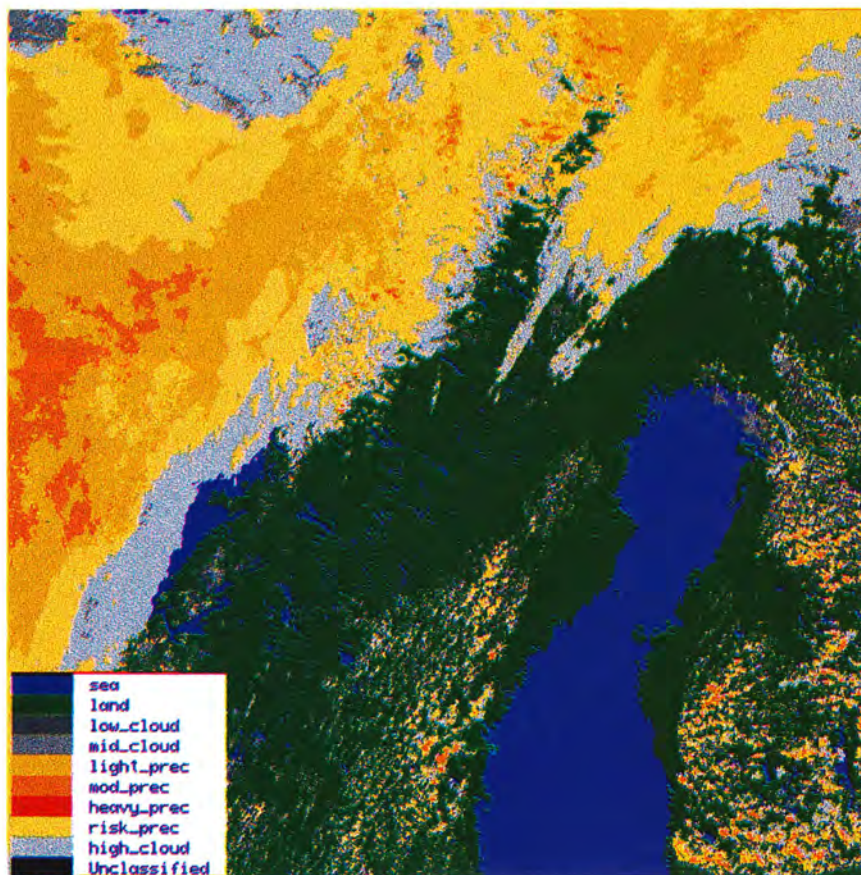


Figure 11. SCANDIA cloud classification presented as precipitation analysis for the same AVHRR scene as in Figures 8-10.

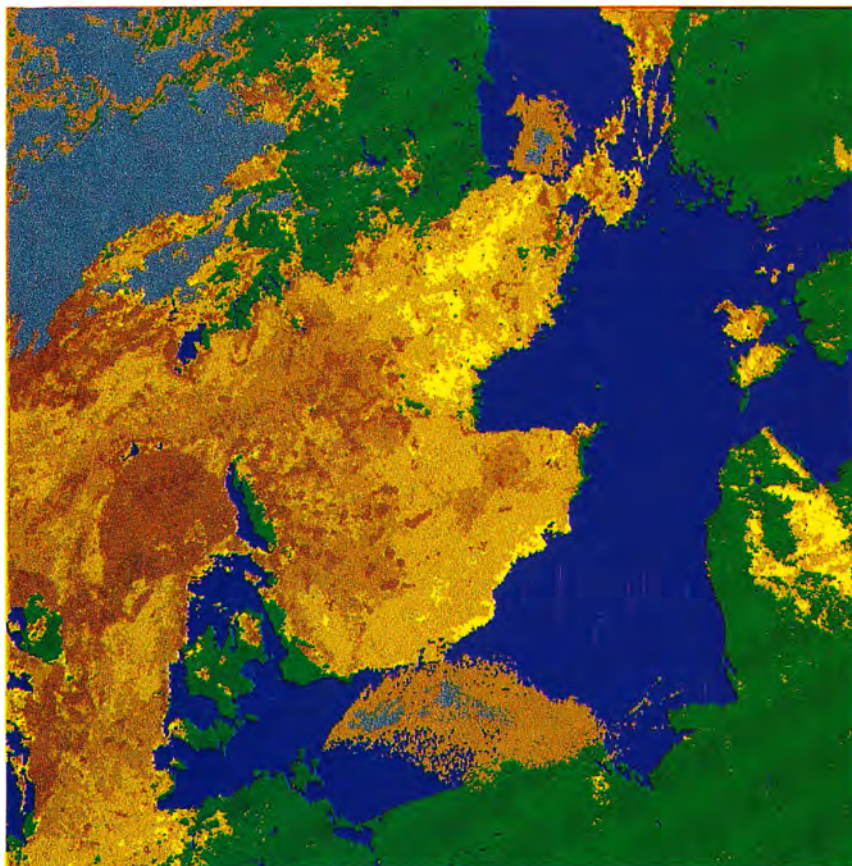


Figure 12. SCANDIA cloud classification presented as a qualitative thickness analysis of low-level clouds from 8 October 1991 at 02:04 UTC. Colour scale ranges from yellow (very thin) to dark red (very thick). Higher clouds are shown in grey.

6. Hydrological applications of the SCANDIA model

Attempts have been made for several years to use SCANDIA results for monitoring of the snow situation in the Swedish mountains above the tree line. The snow situation here is of great importance for the planning of electric power production in Swedish river basins. The area extent of the surface class Snowcover in Table 2 have been estimated and compared to modelled snow magazines and river runoff for selected catchment areas. The HBV-model (described by Bergström, 1992) have been used for these comparisons. Although the snow area extent is not a direct measure of the total snow magazine, it is reasonable to assume a strong correlation between these parameters as long as the snow area extent is not close to 100%.

The method to estimate the area extent of snowcover is simply to compute the fractional coverage of pixels labelled as Snowcover within selected areas. However, this is only possible in situations with very small cloud amounts which naturally limits the amount of usable NOAA satellite scenes.

Figure 13 show results derived from a six-year comparison of SCANDIA-estimated snow area extent and modelled snow magazines during the snowmelting period for the catchment area of Suorva. A reasonable correlation between modelled and observed snow amounts is found. Some problems have been found for smaller catchment areas due to deficiencies in the NOAA scene geometry. It has also been difficult to take into account snow patches (most often classified as Winterforest) which are not fully resolved in NOAA images. More details on these studies are given by Häggström (1994).

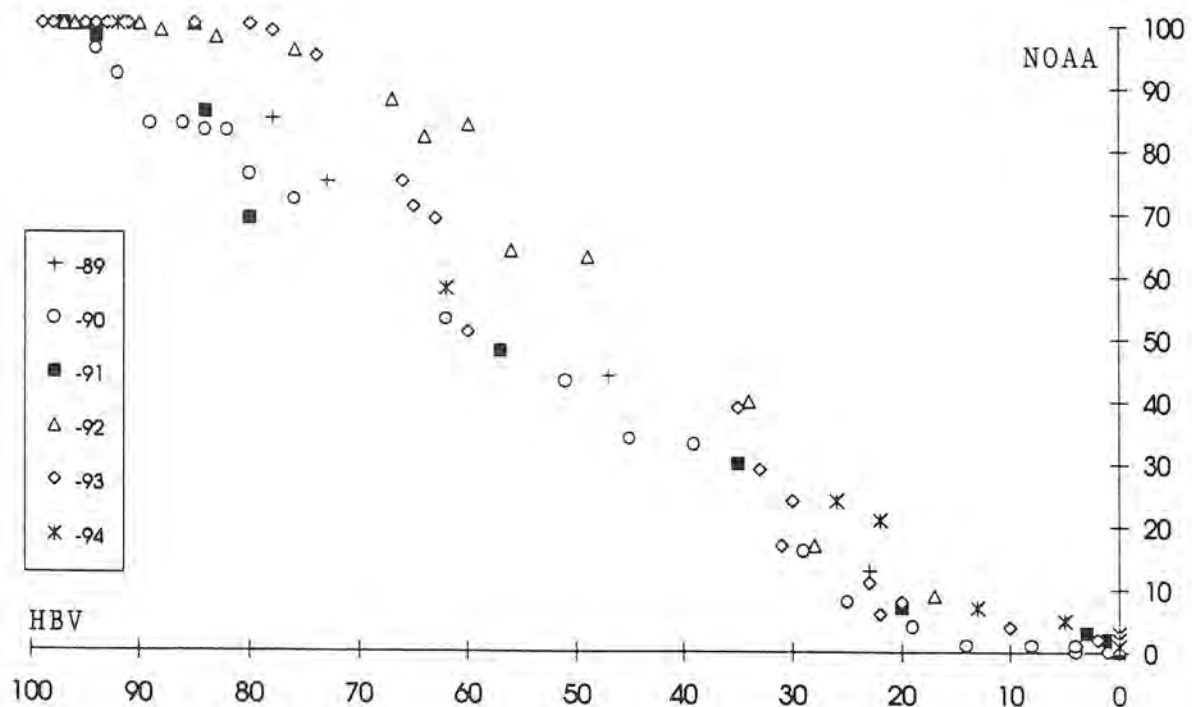


Figure 13. Modelled snow magazine (HBV - in percent of the maximum snow magazine) compared to SCANDIA-estimated snow area extent (NOAA) for the years 1989-1994 in the Suorva catchment area.

7. QUALITY OF SCANDIA CLOUD CLASSIFICATIONS

Considerable experience in the weaknesses and strengths of the SCANDIA model has been gained during the years since the operational implementation of the model in 1988. A special validation experiment (reported by Karlsson, 1993) has been carried out based on comparisons with conventional hourly cloud observations from surface stations (SYNOP). Simultaneous (i.e. with a maximum time difference of 20 minutes) observations of total cloud cover from SYNOP and from satellite were compared for 11 selected SYNOP stations during a two-year period lasting between June 1991 to June 1993. Surface observations were simulated from SCANDIA cloud classifications by computing fractional cloud cover in circular areas surrounding the position of each SYNOP station. According to the classified cloud type, three different radii for the influencing region were chosen in order to compensate for the fact that high-level clouds are generally visible at greater distances than low-level clouds for a surface observer. However, the largest weight was given to the region with the shortest radius (here 15 km). The weights of the three regions were estimated by computing the effective solid angle covered by idealised low-, mid- and high-level clouds of typical heights 1, 4 and 8 km respectively. The principles for these calculations are demonstrated in Figure 14 and more details can be found in Karlsson (1993).

In total, 23 399 comparisons between satellite and SYNOP were collected during the two-year period. Almost 3000 satellite scenes passed the criteria for comparison with SYNOP during the period, which means that approximately 40% of all theoretically available scenes were utilised.

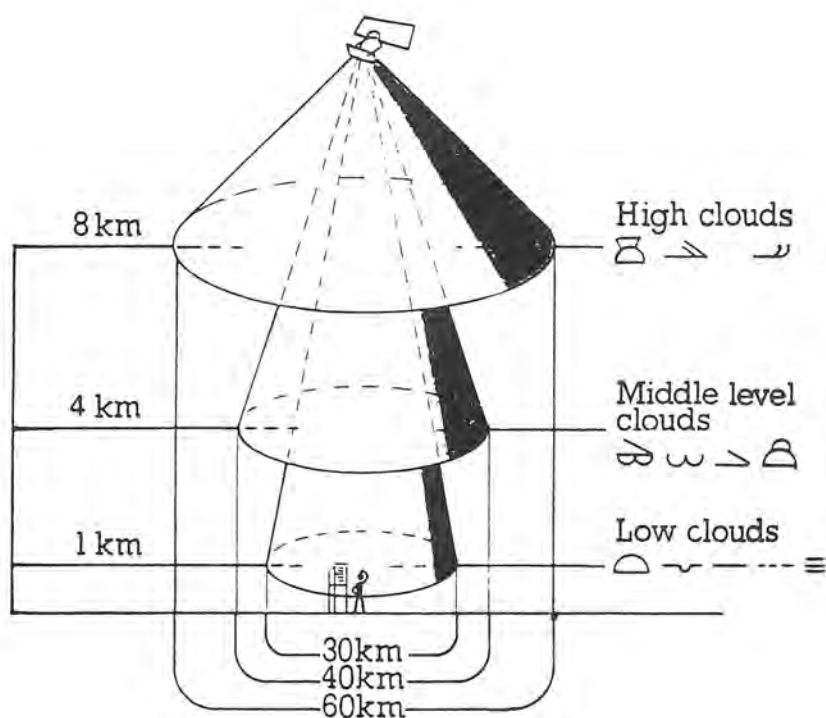


Figure 14. Principle for simulating surface-made cloud observations from SCANDIA cloud classifications. See text and Karlsson (1993) for details.

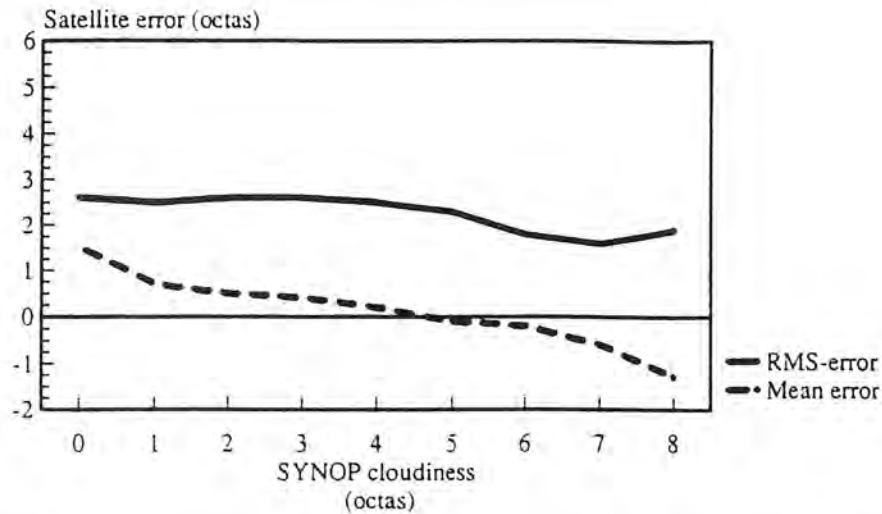


Figure 15. Mean errors and RMS errors (octas) of SCANDIA estimations of total cloud cover compared to SYNOP observations. Results given as a function of SYNOP-reported cloud cover.

Figure 15 shows derived mean errors and root mean squared (RMS) errors as a function of SYNOP-reported cloudiness for the total data set. We conclude that the mean error is close to zero showing that no significant bias exist. However, the RMS errors, varying between 2 and 3 octas, indicate that the variability of the error is quite large. The material was further sub-divided in order to evaluate if the quality of cloud classifications was sensitive to special observation conditions.

A way to summarise these results is to divide the material into groups having different absolute errors. We define four such error groups: 0 - 2 octas, 2 - 4 octas, 4 - 6 octas and 6 - 8 octas. The first group may be seen as the group representing quite an acceptable error. This can be concluded when considering possible sources of error related to the used comparison method and the inherent errors of the SYNOP observations. The two last groups would then contain the worst cases, i.e. when cloudiness is severely overestimated in almost cloud-free conditions or when cloudiness is severely underestimated in cloudy conditions. Table 6 shows the verification results for the following six situations:

- a)* Sun elevations above 10°.
- b)* Sun elevations between -5° and 10°.
- c)* Night conditions.
- d)* Summer conditions (15 May - 15 September).
- e)* Winter conditions (15 November - 15 March).
- f)* All data (15 May 1991 - 20 June 1993).

Table 6. Total distribution of absolute error categories (% of all studied cases) for conditions a-f.

Absolute error category	a)	b)	c)	d)	e)	f)
0-2 octas	86.0%	78.3%	78.5%	83.6%	78.1%	81.4%
2-4 octas	10.5%	14.0%	13.9%	12.8%	13.0%	12.6%
4-6 octas	3.1%	5.8%	5.8%	3.1%	6.5%	4.7%
6-8 octas	0.4%	1.9%	1.8%	0.5%	2.3%	1.3%
Σ samples	9 352	6 764	7 283	7 164	8 658	23 399

For the total data set we notice that 81.4% of the cases have absolute errors less than 2 octas and that errors larger than 4 octas are found in 6% of all cases. It is also seen that results improve during warmer seasons with high sun elevations (conditions *a* and *d*) while results are worse during cold and dark seasons (conditions *b*, *c* and *e*). Nevertheless, seasonal differences are not large which is encouraging and indicative of the usefulness of SCANDIA cloud classifications also during cold and dark seasons.

Validation of classification results focused on individual cloud types was difficult using the SYNOP data set since surface observations very seldomly report single cloud types or single cloud layers with a well-defined cloud amount. Some studies were made for cases with only low-level cloud types reported. Especially interesting here was to investigate the importance of the loss of the brightness temperature difference in feature 4 for low-level water clouds just after sunrise or before sunset. The absence of this typical difference was anticipated to create large separability problems between low-level cloud types and cloud-free regions. Figure 16 shows error characteristics for cases when only low-level cloud types were reported and when sun elevations were restricted to the interval 2-6°. We notice that negative biases as large as 1-2 octas exist for large SYNOP-observed cloud amounts thus confirming that these separability problems do lead to an underestimation of cloud amounts during these special conditions.

The most prominent problem for the SCANDIA model was found in cases with low sun elevations when the AVHRR sensor at the same time was directed towards the sun (i.e. sun-satellite azimuth angles close to 180°) at high satellite zenith angles. Figure 17 shows the extremely poor classification results resulting for cases with sun elevations between 2-6°, satellite zenith angles higher than 45° and sun-satellite azimuth angles higher than 120°. The enhanced forward-scattering from practically all surfaces and objects (earth surfaces, haze, mist and very thin clouds) leads to a dramatic overestimation of cloudiness. Evidently, under these particular conditions the SCANDIA classification can hardly detect cloud-free conditions. Fortunately, only a small fraction of all available AVHRR scenes over Scandinavia suffers from these defects. Most cases are restricted to the morning NOAA passages occurring later than 08 UTC during the spring

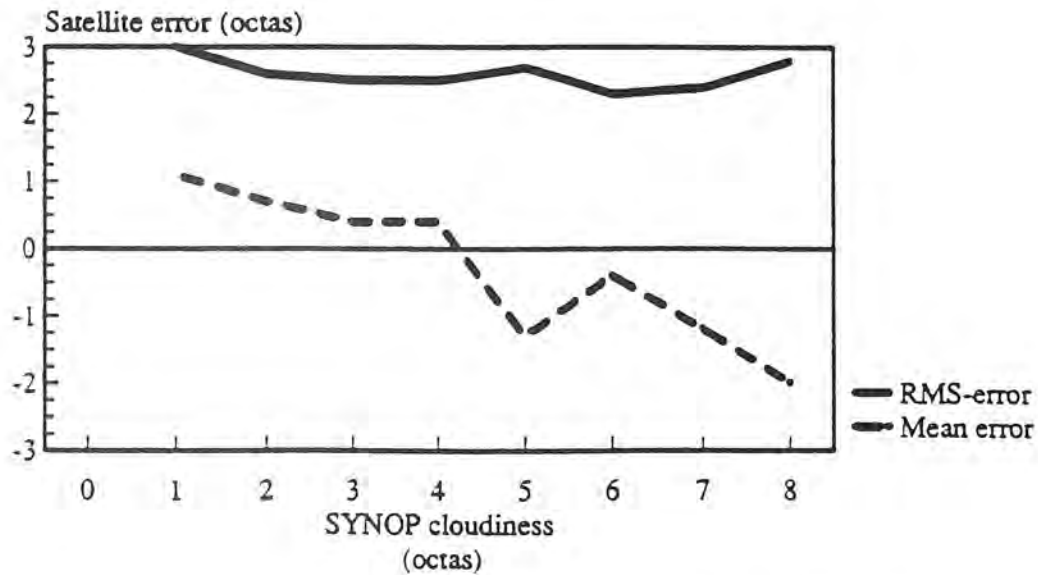


Figure 16. Mean errors and RMS errors (octas) of SCANDIA estimations of total cloud cover for conditions with the following two restrictions: 1. Only low-level cloudiness reported. 2. Sun elevations between 2-6°.

and autumn seasons (satellite passages over the Norwegian Sea and the North Sea just after sunrise).

It was found that not all large differences between satellite and SYNOP were due to weaknesses in the SCANDIA model. E.g., large negative biases were indicated in summer for situations with only convective Cumulus cloudiness present (see Figure 18).

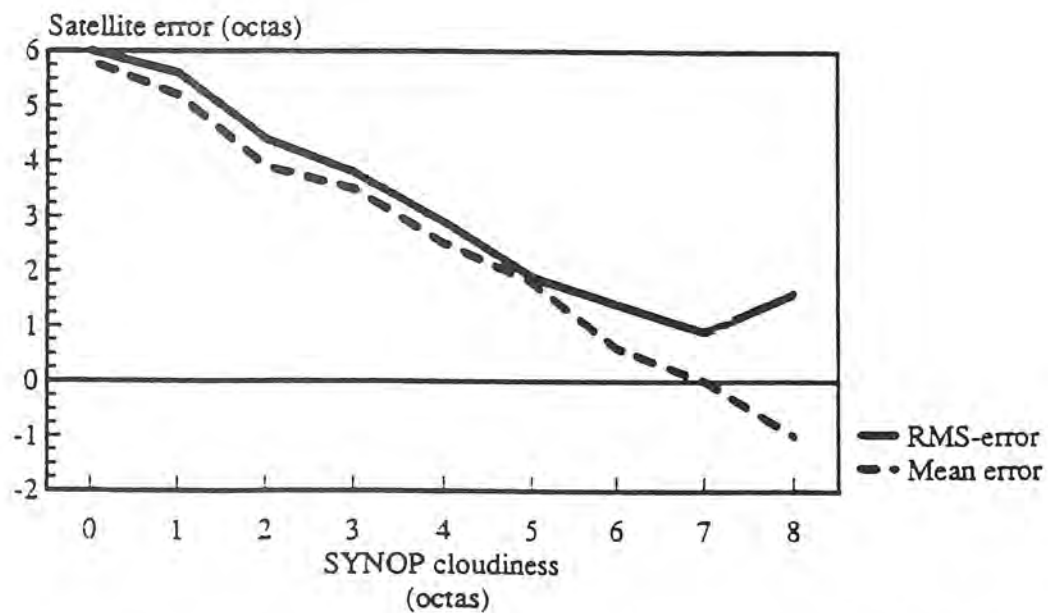


Figure 17. Mean errors and RMS errors for SCANDIA estimations of total cloud cover for conditions with the following three restrictions: 1. Sun elevations interval 2-6°. 2. Satellite-zenith angles below 45°. 3. Sun-satellite azimuth angles larger than 125°.

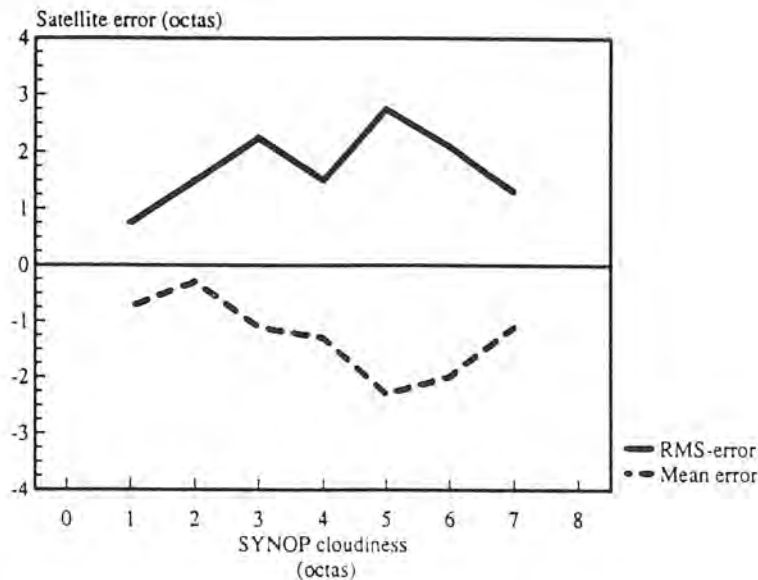


Figure 18. Mean errors and RMS errors (octas) for SCANDIA estimations of total cloud cover for conditions with the following three restrictions; 1. Only Cumulus cloudiness reported in SYNOP. 2. Satellite-zenith angles below 45°. 3. Solar zenith angles above smaller than 80° (sun elevations higher than 10°).

However, it turned out that these differences were to a large extent caused by problems for the surface observer to correctly estimate cloud conditions. Towering Cumulus clouds hide cloud-free portions between cloud elements when an observer views the clouds at off-zenith angles. That this really was the case was concluded from the fact that the bias was very large for low satellite-zenith angles while at higher satellite zenith angles the bias did not exist or it was even reversed in some cases. Another obvious defect of the SYNOP observations was observations of Cirrus cloudiness during dark conditions. Many cases were found where the surface observer reported cloud-free conditions while the satellite analysis showed overcast conditions with Cirrus clouds. Visual inspection of the original AVHRR IR channels did clearly show typical Cirrus shields for most of these situations.

As a summary of factors contributing to the large errors (6% of all samples in Table 6), a list is given below of the most serious defects in the SCANDIA model, along with descriptions of how they affect results.

- Loss of typical brightness temperature differences for clouds in feature 4 near sunrise and sunset.

Causes underestimation of cloudiness and unrealistic appearance of snow- or ice-covered surfaces.

- Extreme anisotropic enhancement of forward-scattering near sunset and sunrise for high satellite zenith angles occurring when the AVHRR sensor is viewing towards the direction of the sun.

Causes severe overestimation of cloudiness, resulting in an excess of low- or mid-level clouds.

- Loss of typical brightness temperature differences for clouds in feature 4 when thin Cirrus clouds are superimposed over low-level clouds, as visualised in Figure 19.

Causes underestimation of cloudiness ("holes" in Cirrus cloud fields).

- Loss of typical brightness temperature differences for clouds in feature 4 when high-level clouds cast shadows on low-level clouds.

Causes underestimation of cloudiness and clouds are often mis-classified as snow and ice surfaces.

- Appearance of AVHRR channel 3 noise, especially in cold winter situations.

Causes both overestimation (stripes with low-level as well as high-level cloud types in cold cloud-free areas) and underestimation (stripes without clouds in evidently overcast areas) of cloudiness.

- Separability problems between cold ground surfaces and mid-level mixed ice/water clouds in cases with strong low-level temperature inversions (i.e. 700 hPa temperatures close to or warmer than surface temperatures - compare with Figure 3).

Causes overestimation of cloudiness with erroneous mid- and high-level clouds.

- Appearance of very strong sunglints.

Causes overestimation of cloudiness over ocean surfaces with erroneous Stratus clouds.

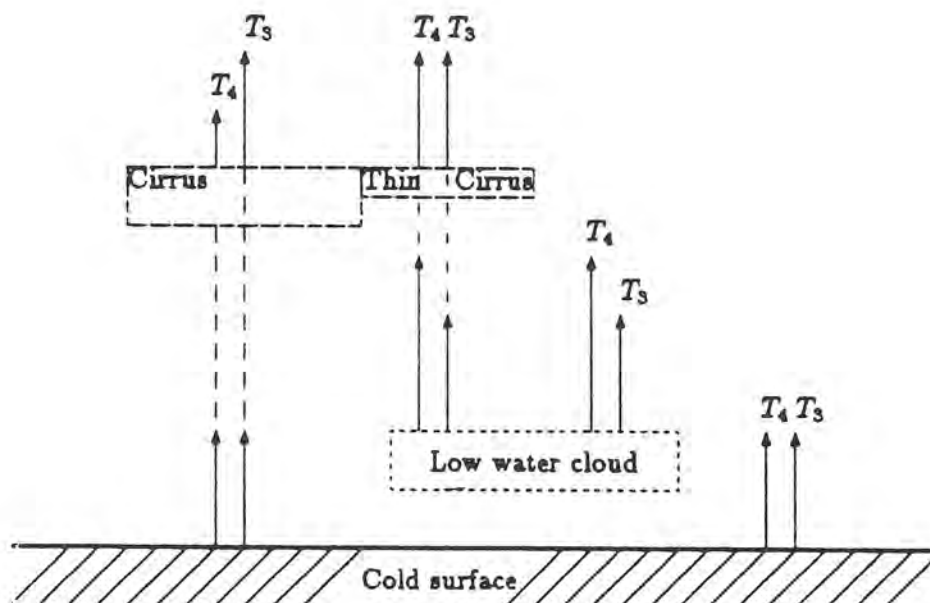


Figure 19. Visualisation of the loss off brightness temperature difference in feature 4 for clouds when thin Cirrus clouds are superimposed over low-level clouds. Length of arrows symbolize Brightness temperatures

- High satellite zenith angles.

Causes overestimation of all cloud types, especially in a moist atmosphere with mist, haze or very thin clouds present.

- Anisotropic enhancement of *back-scattered* solar radiation from wet land areas at high satellite zenith angles.

Causes overestimation of low-level cloudiness. However, a rare occurrence mostly during spring.

For cases when the total cloud cover is correctly estimated by SCANDIA, some errors in the cloud type assignment have been noticed. This has been concluded from the two-year verification data set as well as from operational experience of using SCANDIA classifications in weather forecasting (feedback from forecasters). The most significant defects and their identified causes may be summarised by the following:

- Low-level clouds mis-classified as mid-level clouds in cases with strong low-level temperature inversions.

Caused by separability problems in feature 5 (compare with Figure 3).

- Sub-pixel Cumulus clouds mis-classified as Cirrus clouds.

Caused by separability problems in feature 6.

- Narrow Cirrus sheets or jet contrails mis-classified as Cumulus congestus clouds.

Separability problems in feature 7.

- Stratus clouds mis-classified as Stratocumulus clouds.

Weak separability in feature 7.

- Nimbostratus clouds mis-classified as Altocumulus/Altostratus, Cirrus over Stratus or Cirrus over Altocumulus or vice versa.

Separability problems in feature 5. However, it also reflects a general separability problem due to the possible evaporation of precipitation in lower tropospheric levels (a problem that is relevant also for the interpretation of weather radar imagery).

8. SCANDIA ESTIMATIONS OF CLOUD CLIMATOLOGIES

Despite the fact that a large number of defects and errors in SCANDIA cloud classifications have been noticed, it was shown earlier in the verification study that the errors in estimated cloud amounts were less than two octas in about 80% of all cases (Table 6). When also considering that a large portion of the most grave errors were connected to high satellite viewing angles, we may conclude that if we restrict our use of classifications to only satellite scenes with low satellite viewing angles the estimation of total fractional cloud cover should be quite accurate. This indicates that it should be possible to estimate cloud climatologies (mean of cloud cover) from SCANDIA cloud classifications with a quality comparable with corresponding analyses based on SYNOP observations but with a quite superior horizontal resolution.

Monthly cloud climatologies for the year of 1993 have been estimated and described by Karlsson (1994, 1995_1 and 1996). Monthly cloud climatologies for summer months of 1994 and 1995 have also recently been compiled. Figure 20 shows the resulting mean of cloud cover for the summer and the winter halves of 1993. The summer half of 1993 was defined as the months April to September while the remaining months in 1993 defined the winter half. Only four satellite scenes per day (with the lowest satellite zenith angles at the reception site in Norrköping) were used in order to avoid problems in scenes due to high satellite zenith angles. In this way, the daily cloudiness was estimated from observations at night, in the morning, in the afternoon and in the evening (approximate satellite passage times of NOAA satellites over the area). The mean cloud cover for the month of July is also shown in Figure 21 for the years 1993 and 1994.

The most remarkable features in Figure 20 are the pronounced reduction in cloudiness over ocean and lake areas in summer and the generally higher cloud amounts in the whole area during winter. A minimum cloudiness in winter is found in the central part of Sweden. This is most probably due to a lee effect during the very windy and warm winter months of January, February and March in 1993 with prevailing south-westerly winds (as discussed by Karlsson, 1994). Another particularly interesting feature is the minimum in cloudiness over the Norwegian Sea close to the Norwegian coast during the summer half of 1993. This was found to be correlated with a local minimum in sea surface temperatures occurring in the early summer months (see Karlsson, 1995_1) which most probably was caused by the supply of cold fresh water from the melting snow in the Norwegian mountains. Far off the coast, cloudiness rapidly increases again to very high values. This specific feature was strong enough to be seen in the annual mean cloudiness of the area (Karlsson, 1994 and 1996).

Cloudiness in the July months shown in Figure 21 shows how greatly variable cloud conditions may be for consecutive summers. July 1993 was dominated by a cyclonic weather type while July 1994 had anticyclonic conditions in most places in the area. However, for both months we notice the importance of the ocean and lake areas for reducing cloud amounts.

Comparisons with cloud climatologies created from SYNOP observations (based on 06, 12 and 18 UTC observations) show good agreement with SCANDIA estimations although with a few percent lower cloudiness values for satellite estimations (Karlsson, 1994, and Karlsson, 1996).

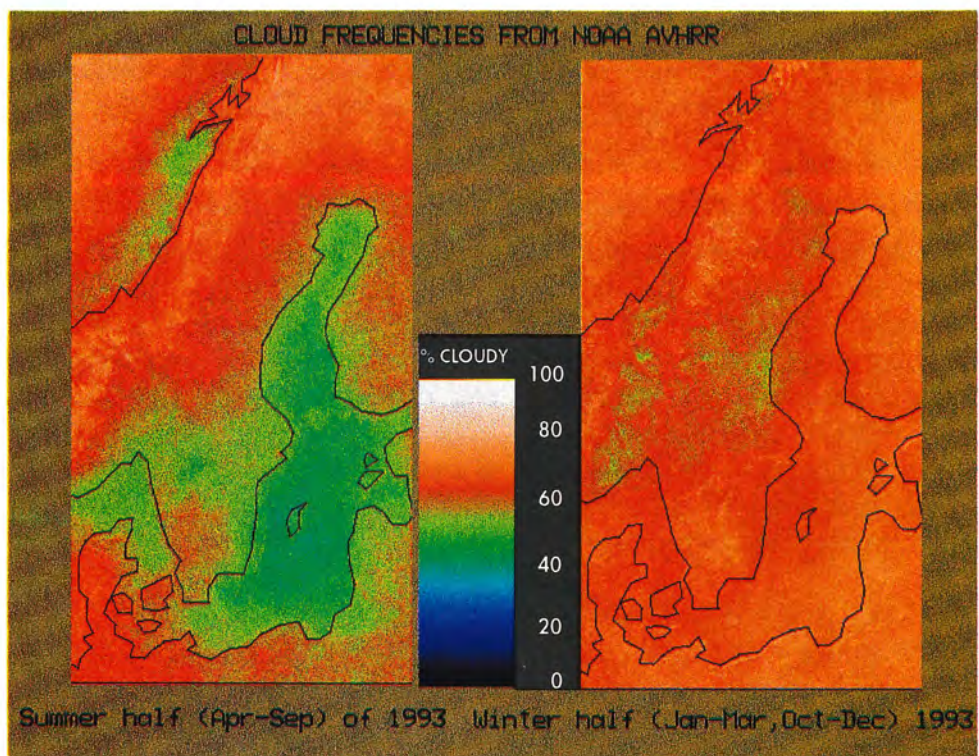


Figure 20. SCANDIA estimations of the mean of cloud cover (in %) in the Nordic area during the summer (left) and winter (right) halves of 1993.

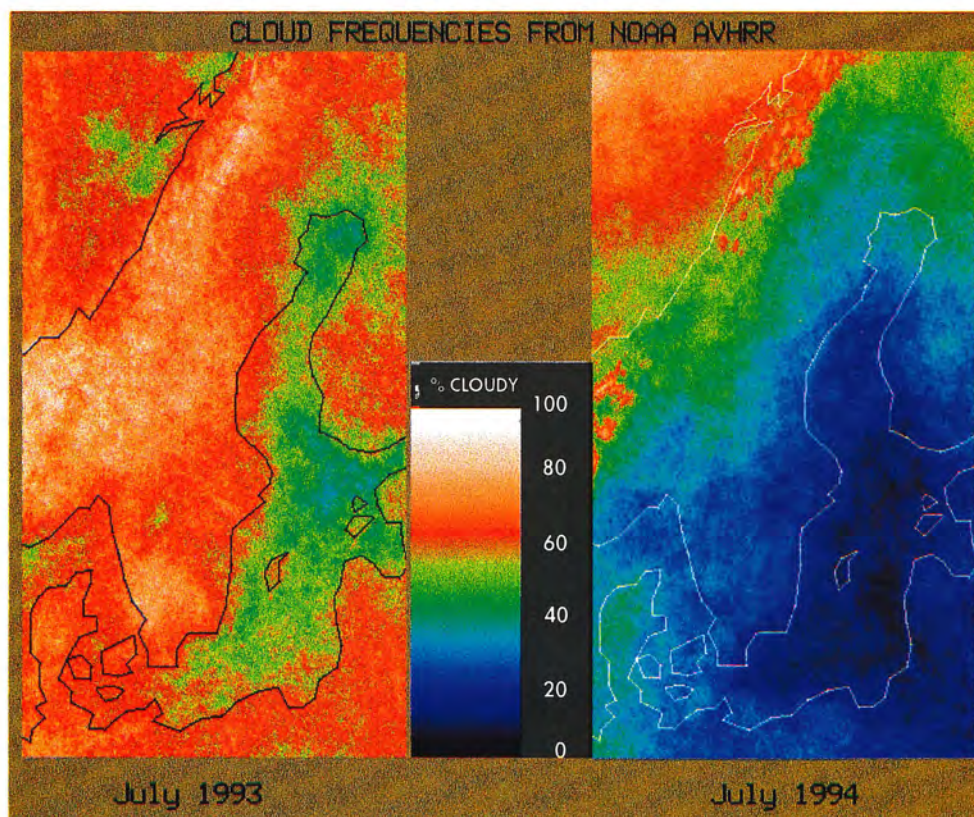


Figure 21. SCANDIA estimations of the mean of cloud cover (in %) in the Nordic area for the month of July in 1993 and in 1994.

9. AN IMPROVED AND MODIFIED SCANDIA MODEL

In order to reduce some of the noticed limitations and defects of SCANDIA cloud classifications and to make classifications possible for larger geographical areas, a new version of the SCANDIA model has been developed. The new version was operationally implemented for an area covering a large part of northern Europe in July 1994.

The most remarkable change from the old SCANDIA scheme is the more accurate treatment of varying sun elevations in the particular area. Instead of using only the sun elevation interval valid at the centre of the area, classifications are now performed for all present sun elevation intervals. The final classification image is then formed by a merging of all cloud classifications defined for each individual image segment having a specific sun elevation interval. A second important change consists of the introduction and use of *a priori* surface temperature information provided by short-range (9-12 hour forecasts) from the HIRLAM (High Resolution Limited Area Model - see Gustafsson, 1991) model. Temperatures in the 700 and 500 hPa levels were further shifted to be based on short-range HIRLAM forecasts and instead of using area means, gridpoint values were now interpolated to the nominal resolution of the particular satellite scene.

The new SCANDIA classifications were not introduced on areas with a maximum horizontal resolution due to constraints in computational demands. Due to this change in horizontal resolution and to a questionable impact on classification results, the textural feature (feature 7 in Table 1) was removed. A summary of the features used in the new SCANDIA version is given in Table 7 below.

Table 7. Classification features used by the new version of the SCANDIA model. Same notation is used as in Table 1.

Feature number	Composition (name)
1	CH1
2	CH1-CH2
3	Land mask
4	CH3-CH4
5	CH4
6	CH5-CH4
7	HIRLAM forecast of 700 hPa temperature (T700)
8	HIRLAM forecast of 500 hPa temperature (T500)
9	HIRLAM forecast of surface temperature (TSUR)

Forecasted surface temperatures are utilised to improve the use of the brightness temperature information in feature 5 for cloud identification in situations where the use of feature 4 is severely restricted (e.g. for very low sun elevations or at night when Cirrus are superimposed over low-level clouds).

If strong temperature inversions are absent near ground (i.e. if forecasted surface temperatures are significantly warmer than the 700 hPa temperature), clouds are identified if feature 5 temperatures are sufficiently colder than the forecasted surface temperature. In situations with forecasted temperature inversions, the pixels are left unclassified with a black colour in the resulting classification image.

In order to further strengthen the protection against misclassifications due to cold surface temperatures, the temperature test in feature 5 is not carried out if surface temperatures below a certain minimum temperature are forecasted. Some compensation is also introduced for apparent warm biases in HIRLAM surface temperature forecasts in very cold situations. A selective filtering of AVHRR channel 3 noise is furthermore performed at cold temperatures. All these tests are based on the use of specific parameters which are listed in Table 8.

Table 8. Important parameters defining dynamic thresholds for the new version of the SCANDIA model.

Parameter	Meaning	Typical values
TEMPADD	Requested minimum temperature difference (feature 5 - feature 9) between surface and clouds for cloud discrimination.	8 K
TSURBIAS	Compensation for bias in HIRLAM surface temperature forecasts (too warm in extremely cold situations at present). Surfaces colder than (T700+TSURBIAS) blacklisted to avoid confusion with middle level clouds in cold winter situations.	10 K
COLDLAND	Cloud tests using TEMPADD excluded for surfaces colder than COLDLAND (in cold winter situations) in feature 9.	270 K
NOISETEMP	Noise filtering by a 5x5 pixel wide low-pass filter. Performed in feature 4 for areas colder than NOISETEMP in feature 9.	277 K

It is also important to notice that the use of forecasted surface temperatures has replaced the use of most of the temperature parameters listed in Table 5. This means that instead of using within-season static thresholds, dynamic temperature thresholds are now used which are tuned to the present weather situation as described by HIRLAM forecasts.

The introduction of unclassified black pixels in the result image has been included in order to alert the forecaster to the possibility of severe separability problems during special circumstances. An extra feature here is that all pixels that are classified as cloud-free in the sun elevation interval 0-5° are *always* coloured black in order to display to the forecaster where the critical zone near sunrise and sunset appears in the image. Black-listed pixels may also occur at higher sun-elevations as a result of shadows that are cast on lower level clouds by high-level clouds, thus removing the typical daytime signature of clouds in feature 4. These shadows will however be correctly classified in the absence of forecasted temperature inversions when cloud top temperatures differ significantly (as defined by parameter TEMPADD in Table 8) from the surface temperature.

The interpretation of the black areas appearing in the classification images is thus that there is an increased risk of misclassification of these pixels. The forecaster must then use other observations or (if he/she is very skilled in image interpretation) use original NOAA images with caution. In some situations, especially during cold winter situations, very large areas will be coloured black in the classification images (mainly because of the risk of mistaking cold ground surfaces for mid-level cloudiness). However, in general only a small fraction of these black pixels are really clouds and not cloud-free land or sea (ice) surfaces.

Figures 22 and 23 show two examples of the new SCANDIA cloud classifications. Figure 22 shows a typical classification in good illumination conditions and Figure 23 a more problematic situation with very low sun elevations occurring in the area as well as completely dark regions with very cold ground temperatures. Notice how blacklisted pixels indicate the zone of sunrise and areas with very cold ground temperatures. The wavy edge of the zone of twilight is appearing due to simplifications in the computation of the sun elevation at each pixel position for optimisation reasons.

The operational experience has so far been very encouraging. The subjective validation of the new SCANDIA classifications indicates that they are most often more accurate than the original classifications that are still run on the areas with high horizontal resolution. This has also been verified from comparisons of monthly cloud climatologies on this larger geographical area with SYNOP-derived climatologies and with climatologies based on the original classification on areas with high horizontal resolution.

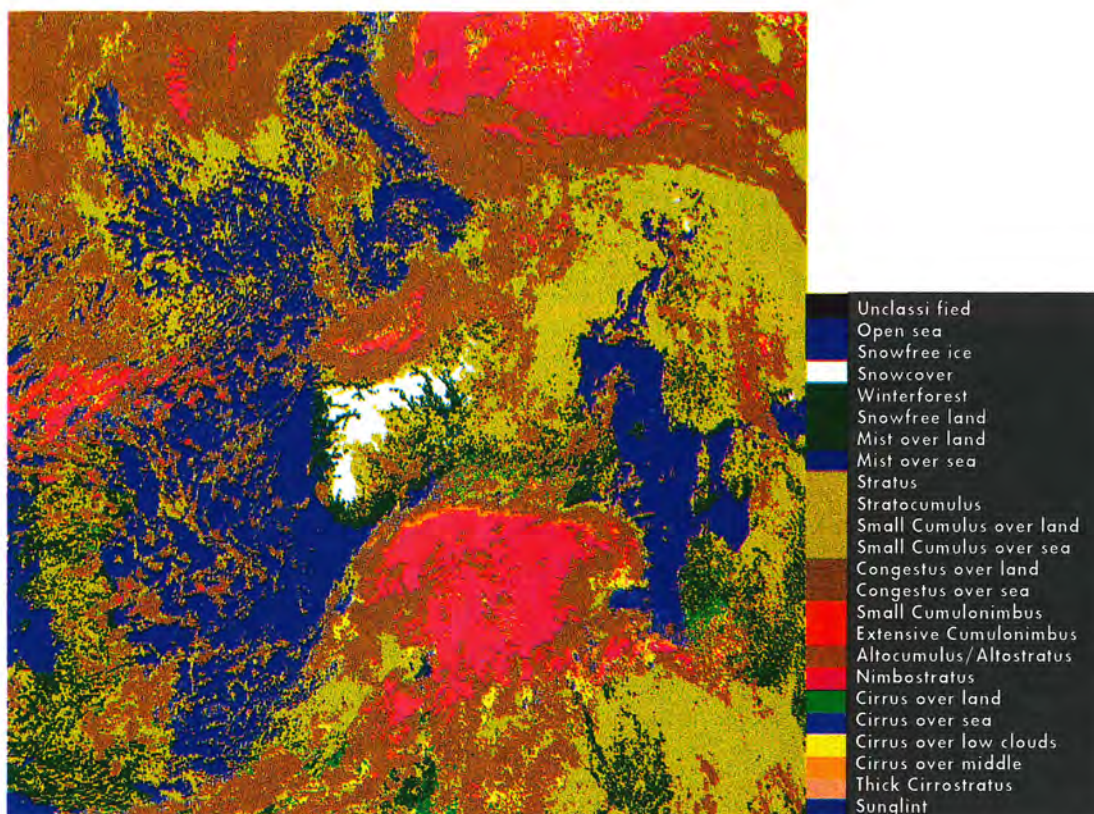


Figure 22. New version of SCANDIA cloud classification over the Scandinavian and north European region for an AVHRR scene from 18 April 1995 at 11:54 UTC.

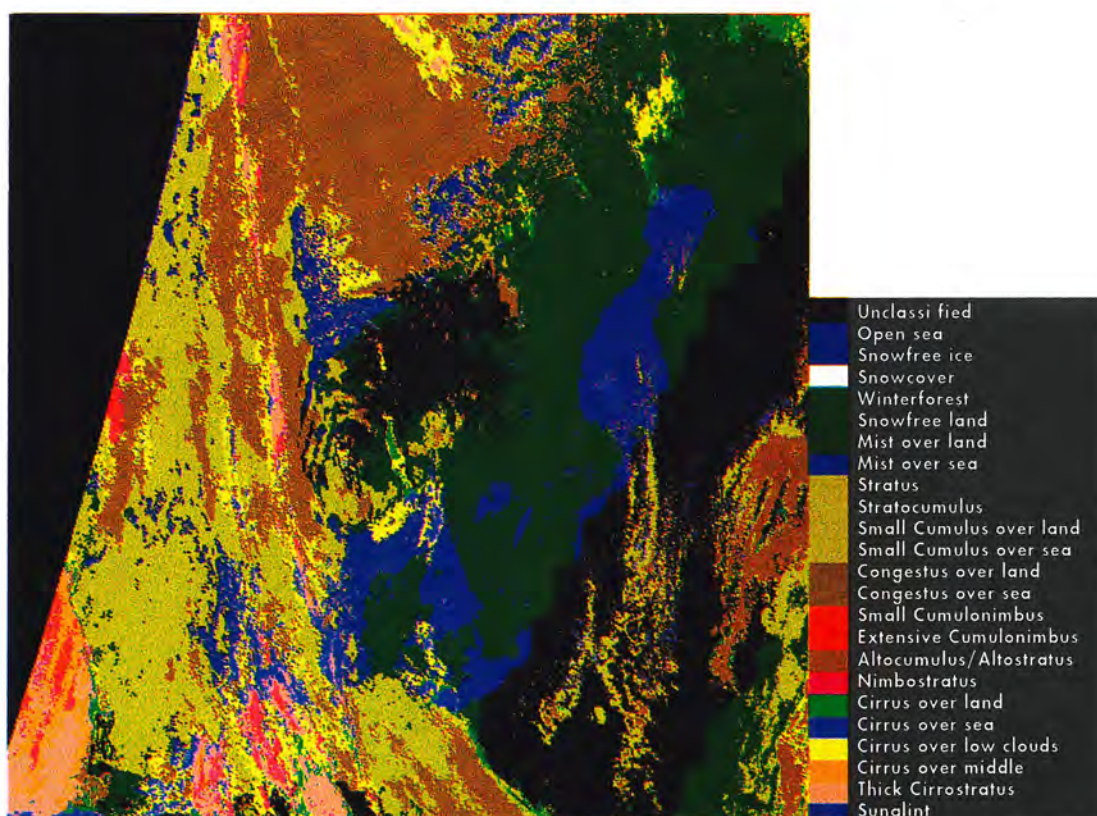


Figure 23. New version of SCANDIA cloud classification for an AVHRR scene from November 1995 at 06:35 UTC. Notice the black zone of sunrise (where low-level cloudiness may be underestimated) and the black region with cold ground temperatures (where mid- and high-level cloudiness may be underestimated).

10. Model validation applications

The new SCANDIA version has been successfully used in NWP model validation experiments (Karlsson, 1995_2) where the description and spin-up of cloudiness in various models have been studied. Forecasts of total fractional cloud cover were studied for several forecast lead times for the HIRLAM and ECMWF models (see Acronym list). The comparisons were made with SCANDIA monthly cloud climatologies since the synoptic NOAA passage times make direct forecast-to-scene comparisons very cumbersome. Significant underestimation of cloud amounts (exceeding 10% in value) was found for both the ECMWF and HIRLAM models. For the HIRLAM model, the underestimation was large and almost unchanged also for longer forecasts (e.g. 48 hours).

More recent studies have shown substantial improvements of HIRLAM cloud forecasts after the introduction of a simple cloud initialisation technique. This technique is based on the use of six-hour forecasts of clouds (so called "first-guess" fields) in the HIRLAM analysis process. Table 9 show validation results for HIRLAM forecasts with five different lead times and Figures 24 and 25 show the SCANDIA-analysed and HIRLAM-forecasted (from 24-hour forecasts) cloud climatology respectively for the month of March in 1995. It is seen that the bias in forecasted cloud amounts is now very small for forecast lead times longer than 24-hours. However, underestimation of cloud amounts is still evident for short forecast lead times.

Table 9. Area mean of monthly cloud cover for March 1994 from HIRLAM forecasts (denoted HIR) of varying lead times compared to SCANDIA-estimated cloud cover. Resulting mean error and RMS error of the monthly mean are also shown. Same area is used as in Figures 24 and 25.

MARCH 1995 - Initialized clouds
(Initial cloud water and cloud cover from 6-hour forecasts)

	Satellite	HIR +06h	HIR +12h	HIR +24h	HIR +36h	HIR +48h
Cloudiness (%)	68.2	58.5	63.5	67.4	69.5	70.6
Bias (%)		-9.7	-4.7	-0.8	1.3	2.4
RMS (%)		11.0	6.8	5.2	5.7	5.6

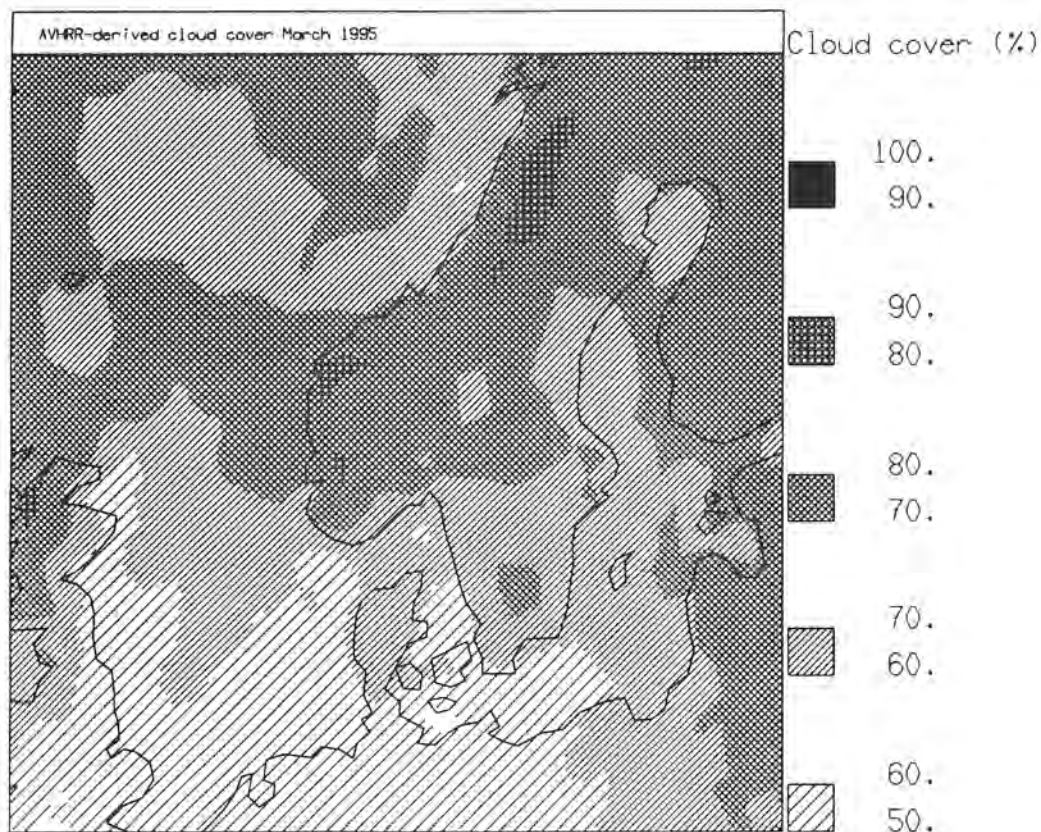


Figure 24. SCANDIA-derived mean of cloud cover (%) for March 1995 in the north European area. Horizontal resolution 55 km.

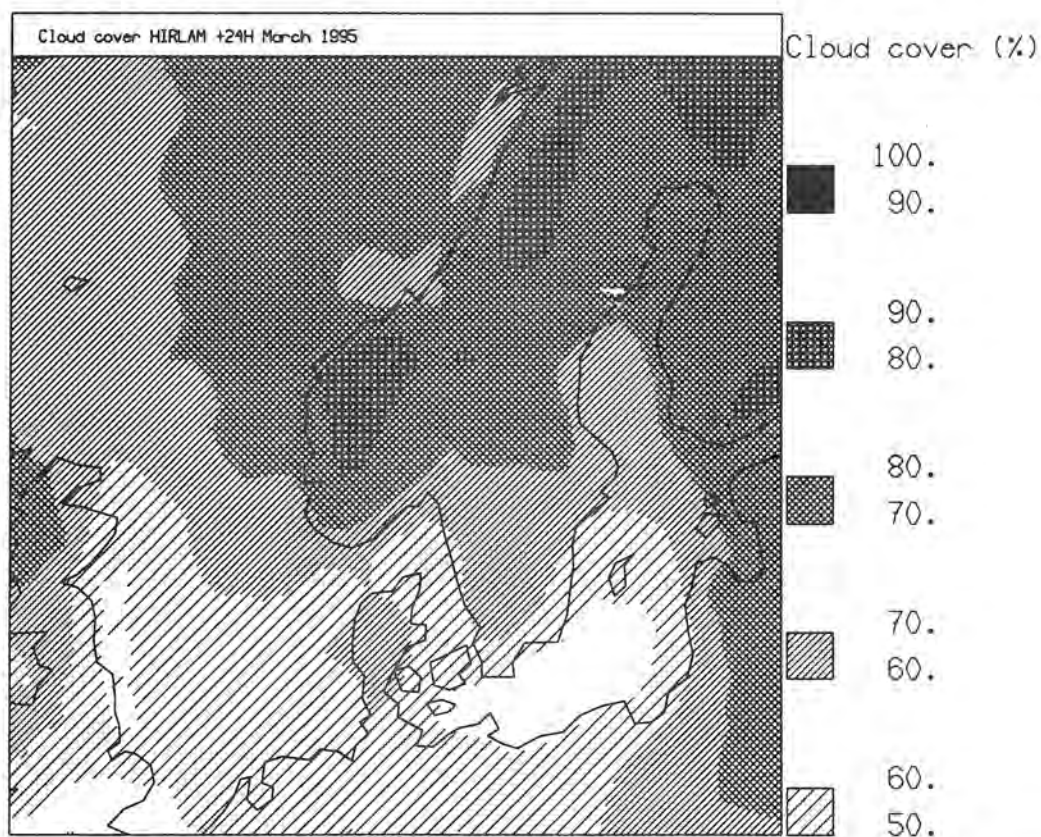


Figure 25. Mean of cloud cover (%) in March 1995 from HIRLAM 24-hour forecasts for same area and horizontal resolution as in Figure 24.

11. Future plans

A goal for the near future is to replace the original SCANDIA model with the new version run at maximum horizontal resolution on a large geographical area. A shift to a more continuous change of thresholds as a function of sun elevation is also planned as well as actions to compensate for extreme anisotropic reflection. Errors caused by extreme anisotropic reflection at very low sun elevations are serious and severely limit the use of SCANDIA results during the winter season for satellite scenes with high satellite-zenith viewing angles.

However, much effort must first be made in investigating how to limit the possible risk of degrading cloud classification results by using NWP forecasts directly in the classification process. The used HIRLAM surface temperatures are obviously influenced by internal model errors in the description of cloud parameters (errors in cloud locations, cloud amounts and cloud types/layers). This fact has enforced a rather large value of the parameter TEMPADD (see Table 8) in order to reduce the effect of large errors in forecasted surface temperatures. Unfortunately, this action also reduces the realised improvement of classifications in cold winter situations.

Another problem is to include a realistic description of the well-known small-scale variation of surface temperatures that is not given by the HIRLAM forecasts. The present technique has led to some overestimation of cloud cover in mountainous areas where the small-scale temperature variation is very large.

The *a priori* surface temperature information is nevertheless crucial for the future improvement and success of any cloud classification model. Hopefully, surface temperature analysis schemes may provide near-real time temperature analyses in the future thus enabling a removal of the dependence on the accuracy of short-term temperature forecasts. Furthermore, other auxiliary information (e.g. lower tropospheric moisture analyses, snow- and ice analyses etc.) should be of great value in future development of cloud classification models.

A more systematic use of the SCANDIA model for cloud climate studies and for NWP model validation experiments is planned at SMHI, partly as a contribution to the BALTEX research programme. Especially the effects on the cloud forecasts when increasing the horizontal and vertical HIRLAM resolution will be studied. Furthermore, cloud climate data over the Nordic area will be compiled for the period 1991-1998 in a research project sponsored by the Swedish National Space Board. This new data set will not be contaminated by any model data since it will be based on results from the original SCANDIA model. In parallel, similar cloud climate analyses will be compiled for the years 1994 to 1998 from the latest version of the SCANDIA model including *a priori* temperature information from HIRLAM forecasts. Thus, comparisons of the two data sets and conventional cloud climate information from SYNOP observations will then be possible. This should indicate if the quality of analysed cloud amounts does improve significantly when utilising *a priori* temperature information from HIRLAM forecasts.

ACKNOWLEDGEMENTS

The author is greatly indebted to Erik Liljas for initiating this work in the field of automatic satellite image interpretation at SMHI. He has also contributed with several figures in the report and has given valuable comments on the manuscript. The author also thanks Daniel Michelson for correcting the manuscript, Mats Moberg for giving valuable comments and Eva-Lena Ljungkvist for assisting with some of the figures.

ACRONYMS

APOLLO	AVHRR Processing scheme Over cLoud, Land and Ocean
AVHRR	Advanced Very High Resolution Radiometer (NOAA satellite).
BALTEX	BALTic sea EXperiment (GEWEX activity)
CMS	Centre Meteorologie Spatial (Lannion, France)
ECMWF	European Centre for Medium range Weather Forecasts, Reading, U.K.
GEWEX	Global Energy and Water cycle EXperiment
HIRLAM	High Resolution Limited Area Model - NWP model developed by the Meteorological Institutes in the Nordic countries plus Ireland, the Netherlands and Spain.
IR	InfraRed part of electromagnetic spectrum.
MSG	METEOSAT Second Generation
NOAA	National Oceanic and Atmospheric Administration (USA).
NWP	Numerical Weather Prediction
RGB	Red, Green, Blue. Colour components for multispectral images.
SCANDIA	SMHI Cloud Analysis model using Digital AVHRR data
SEVIRI	Spinning Enhanced Visible and Infra-Red Imager (MSG)
SMHI	Swedish Meteorological and Hydrological Institute
SYNOP	SYNOptical weather observations at surface stations
VIS	Visible part of electromagnetic spectrum.

REFERENCES

- Allam, R.J, Holpin, G., Jacksson, P. and Liberti, G.-L. (1993)
GPCP AIP-2 Workshop Report, 23-26 August 1993, Shinfield Park, Reading, UK.
Available from UK Meteorological Office.
- Arking, A. and Childs, J.D. (1985)
Retrieval of cloud cover parameters from multispectral satellite measurements.
J. Clim. Appl. Meteor., 24, 322-333.
- Bergström, S. (1992)
The HBV Model - its structure and applications.
SMHI Report Hydrology, No. 4.
- Coakley, J.A. and Bretherton, F.P. (1982)
Cloud cover from high resolution scanner data: detecting and allowing for partially filled views of view.
J. Geophys. Res., 87, 4917-4932.
- Derrien, M., Farki, B., Harang, L., LeGléau, H., Noyalet, A., Pochic, D. and Sairouni, A. (1993)
Automatic cloud detection applied to NOAA-11/AVHRR imagery.
Rem. Sens. of Env., 46, 246-267.
- Desbois, M., Seze, G. and Szejwach, G. (1982)
Automatic classification of clouds in METEOSAT imagery: Application to high-level clouds.
J. Appl. Meteor., 21, 401-412.
- Dybbroe, A. (1995)
Cloud classification with AVHRR data (in Danish).
Tech. Rep. 95-3, Danish Meteorological Institute, 70 pp.
- d'Entremont, R.P. (1986)
Low- and mid-level cloud analysis using nighttime multispectral imagery.
J. Clim. Appl. Meteor., 25, 1853-1869.
- Eyre, J.R., Brownscombe, J.L. and Allam, R.J. (1984)
Detection of fog at night using Advanced Very High Resolution Radiometer (AVHRR) imagery.
Meteor. Mag., 113, 266-271.
- Gustafsson, N. (1991)
The HIRLAM model.
In Proc. Seminar on Numerical Methods in Atmospheric Models, ECMWF, Reading, UK, 9-13 Sep. 1991, 115-146.
- Häggström, M. (1994)
Monitoring the snow area extent in the Swedish mountains from NOAA AVHRR images (in Swedish).
SMHI Report Hydrology, No. 57, 43 pp.

- Inoue, T. (1987)
Cloud type classification with NOAA-7 split window measurements.
J. Geophys. Res., 92, 3991-4000.
- Karlsson, K.-G. (1989)
Development of an operational cloud classification model.
Int. J. Remote Sens., 10, 687-693.
- Karlsson, K.-G. (1993)
Comparison of operational AVHRR-based cloud analyses with surface observations.
In Proc. 6th European AVHRR Data Users' Meeting, Belgirate, Italy, 28 June - 3 July, 1993, EUMETSAT, 223-230.
- Karlsson, K.-G. (1994)
Satellite-estimated cloudiness from NOAA AVHRR data in the Nordic area during 1993.
SMHI Reports Meteorology and Climatology, No. 66, 51 pp.
- Karlsson, K.-G. (1995_1)
Estimation of cloudiness at high latitudes from multispectral satellite measurements.
Ambio, 24, 33-40.
- Karlsson, K.-G. (1995_2)
Validation of HIRLAM cloud cover forecasts using satellite-derived cloud cover statistics.
In Proc. of ECMWF/GEWEX Workshop on Modelling, validation and assimilation of clouds, Reading, UK, 31 Oct - 4 Nov 1994, 263-276.
- Karlsson, K.-G. (1996)
Cloud climate investigations in the Nordic region using NOAA AVHRR data.
Submitted to J. Appl. Theor. Climatology.
- Karlsson, K.-G. and Liljas, E. (1990)
The SMHI model for cloud and precipitation analysis from multispectral AVHRR data.
SMHI PROMIS Reports, No. 10, 74 pp.
- Liljas, E. (1982)
Automated techniques for the analysis of satellite cloud imagery.
In Nowcasting, Ed. K. A. Browning, Academic Press, 177-190.
- Liljas, E. (1984)
Processed satellite imageries for operational forecasting.
Swedish Meteorological and Hydrological Institute/Swedish Space Corporation, 43 pp.
- Liljas, E. (1986)
Use of the AVHRR 3.7 micrometer channel in multispectral cloud classification.
SMHI PROMIS Reports, No. 2, 23 pp.
- Raustein, E. (1989)
Use of a clustering method for objective cloud classification and determination of cloud parameters from satellite data.
Report NR:2, Meteorological Report Series, University of Bergen, 19 pp.

Saunders, R.W. and Kriebel, K.T. (1988)

An improved method for detecting clear sky and cloudy radiances from AVHRR data.
Int. J. Rem. Sens., 9, 123-150.

Setvak, M. and Doswell, C.A. (1991)

The AVHRR channel 3 cloud top reflectivity of convective storms.
Mon. Wea. Rev., 119, 841-847.

SMHI's publications

SMHI publishes six report series. Three of these, the R-series, are intended for international readers and in most cases written in English. For the others the Swedish language is used.

Names of the Series	Published since
RMK (Report Meteorology och Climatology)	1974
RH (Report Hydrology)	1990
RO (Report Oceanography)	1986
METEOROLOGI	1985
HYDROLOGI	1985
OCEANOGRAFI	1985

Earlier issues published in serie RMK

- | | |
|---|---|
| <p>1 Thompson, T., Udin, I., and Omstedt, A. (1974)
Sea surface temperatures in waters surrounding Sweden.</p> <p>2 Bodin, S. (1974)
Development on an unsteady atmospheric boundary layer model.</p> <p>3 Moen, L. (1975)
A multi-level quasi-geostrophic model for short range weather predictions.</p> <p>4 Holmström, I. (1976)
Optimization of atmospheric models.</p> <p>5 Collins, W.G. (1976)
A parameterization model for calculation of vertical fluxes of momentum due to terrain induced gravity waves.</p> <p>6 Nyberg, A. (1976)
On transport of sulphur over the North Atlantic.</p> <p>7 Lundqvist, J.-E., and Udin, I. (1977)
Ice accretion on ships with special emphasis on Baltic conditions.</p> <p>8 Eriksson, B. (1977)
Den dagliga och årliga variationen av temperatur, fuktighet och vindhastighet vid några orter i Sverige.</p> | <p>9 Holmström, I., and Stokes, J. (1978)
Statistical forecasting of sea level changes in the Baltic.</p> <p>10 Omstedt, A., and Sahlberg, J. (1978)
Some results from a joint Swedish-Finnish sea ice experiment, March, 1977.</p> <p>11 Haag, T. (1978)
Byggnadsindustrins väderberoende, seminarieuppsats i företagsekonomi, B-nivå.</p> <p>12 Eriksson, B. (1978)
Vegetationsperioden i Sverige beräknad från temperaturobservationer.</p> <p>13 Bodin, S. (1979)
En numerisk prognosmodell för det atmosfäriska gränsskiktet, grundad på den turbulenta energiekvationen.</p> <p>14 Eriksson, B. (1979)
Temperaturfluktuationer under senaste 100 åren.</p> <p>15 Udin, I., och Mattisson, I. (1979)
Havsis- och snöinformation ur datorbearbetade satellitdata - en modellstudie.</p> <p>16 Eriksson, B. (1979)
Statistisk analys av nederbördsdata. Del I. Arealnederbörd.</p> <p>17 Eriksson, B. (1980)
Statistisk analys av nederbördsdata. Del II. Frekvensanalys av månadsnederbörd.</p> |
|---|---|

- 18 Eriksson, B. (1980)
Årsmedelvärden (1931-60) av nederbörd, avdunstning och avrinning.
- 19 Omstedt, A. (1980)
A sensitivity analysis of steady, free floating ice.
- 20 Persson, C., och Omstedt, G. (1980)
En modell för beräkning av luftföroreningars spridning och deposition på mesoskala.
- 21 Jansson, D. (1980)
Studier av temperaturinversioner och vertikal vindskjuvning vid Sundsvall-Härnösands flygplats.
- 22 Sahlberg, J., and Törnevik, H. (1980)
A study of large scale cooling in the Bay of Bothnia.
- 23 Ericson, K., and Hårsmar, P.-O. (1980)
Boundary layer measurements at Klockrike. Oct. 1977.
- 24 Bringfelt, B. (1980)
A comparison of forest evapotranspiration determined by some independent methods.
- 25 Bodin, S., and Fredriksson, U. (1980)
Uncertainty in wind forecasting for wind power networks.
- 26 Eriksson, B. (1980)
Graddagsstatistik för Sverige.
- 27 Eriksson, B. (1981)
Statistisk analys av nederbördsdata. Del III. 200-åriga nederbördsserier.
- 28 Eriksson, B. (1981)
Den "potentiella" evapotranspirationen i Sverige.
- 29 Pershagen, H. (1981)
Maximisnödjun i Sverige (perioden 1905-70).
- 30 Lönnqvist, O. (1981)
Nederbördsstatistik med praktiska tillämpningar.
(Precipitation statistics with practical applications.)
- 31 Melgarejo, J.W. (1981)
Similarity theory and resistance laws for the atmospheric boundary layer.
- 32 Liljas, E. (1981)
Analys av moln och nederbörd genom automatisk klassning av AVHRR-data.
- 33 Ericson, K. (1982)
Atmospheric boundary layer field experiment in Sweden 1980, GOTEX II, part I.
- 34 Schoeffler, P. (1982)
Dissipation, dispersion and stability of numerical schemes for advection and diffusion.
- 35 Undén, P. (1982)
The Swedish Limited Area Model. Part A. Formulation.
- 36 Bringfelt, B. (1982)
A forest evapotranspiration model using synoptic data.
- 37 Omstedt, G. (1982)
Spridning av luftförorening från skorsten i konvektiva gränsskikt.
- 38 Törnevik, H. (1982)
An aerobiological model for operational forecasts of pollen concentration in the air.
- 39 Eriksson, B. (1982)
Data rörande Sveriges temperaturklimat.
- 40 Omstedt, G. (1984)
An operational air pollution model using routine meteorological data.
- 41 Persson, C., and Funkquist, L. (1984)
Local scale plume model for nitrogen oxides. Model description.
- 42 Gollvik, S. (1984)
Estimation of orographic precipitation by dynamical interpretation of synoptic model data.
- 43 Lönnqvist, O. (1984)
Congression - A fast regression technique with a great number of functions of all predictors.
- 44 Laurin, S. (1984)
Population exposure to SO_2 and NO_x from different sources in Stockholm.
- 45 Svensson, J. (1985)
Remote sensing of atmospheric temperature profiles by TIROS Operational Vertical Sounder.

- 46 Eriksson, B. (1986)
Nederbörds- och humiditetsklimat i Sverige under vegetationsperioden.
- 47 Taesler, R. (1986)
Köldperioden av olika längd och förekomst.
- 48 Wu Zengmao (1986)
Numerical study of lake-land breeze over Lake Vättern, Sweden.
- 49 Wu Zengmao (1986)
Numerical analysis of initialization procedure in a two-dimensional lake breeze model.
- 50 Persson, C. (1986)
Local scale plume model for nitrogen oxides. Verification.
- 51 Melgarejo, J.W. (1986)
An analytical model of the boundary layer above sloping terrain with an application to observations in Antarctica.
- 52 Bringfelt, B. (1986)
Test of a forest evapotranspiration model.
- 53 Josefsson, W. (1986)
Solar ultraviolet radiation in Sweden.
- 54 Dahlström, B. (1986)
Determination of areal precipitation for the Baltic Sea.
- 55 Persson, C. (SMHI), Rodhe, H. (MISU), De Geer, L.-E. (FOA) (1986)
The Chernobyl accident - A meteorological analysis of how radionuclides reached Sweden.
- 56 Persson, C., Robertsson, L. (SMHI), Grennfelt, P., Kindbom, K., Lövblad, G., och Svanberg, P.-A. (IVL) (1987)
Luftföroreningsepisoden över södra Sverige 2 - 4 februari 1987.
- 57 Omstedt, G. (1988)
An operational air pollution model.
- 58 Alexandersson, H., Eriksson, B. (1989)
Climate fluctuations in Sweden 1860 - 1987.
- 59 Eriksson, B. (1989)
Snödjupsförhållanden i Sverige - Säsongerna 1950/51 - 1979/80.
- 60 Omstedt, G., Szegő, J. (1990)
Människors exponering för luftföroreningar.
- 61 Mueller, L., Robertson, L., Andersson, E., Gustafsson, N. (1990)
Meso- γ scale objective analysis of near surface temperature, humidity and wind, and its application in air pollution modeling.
- 62 Andersson, T., Mattisson, I. (1991)
A field test of thermometer screens.
- 63 Alexandersson, H., Gollvik, S., Mueller, L. (1991)
An energy balance model for prediction of surface temperatures.
- 64 Alexandersson, H., Dahlström, B. (1992)
Future climate in the Nordic region - survey and synthesis for the next century.
- 65 Persson, C., Langner, J., Robertson, L. (1994)
Regional spridningsmodell för Göteborgs och Bohus, Hallands och Älvsborgs län. (A mesoscale air pollution dispersion model for the Swedish west-coast region. In Swedish with captions also in English.)
- 66 Karlsson, K.-G. (1994)
Satellite-estimated cloudiness from NOAA AVHRR data in the Nordic area during 1993.



Swedish Meteorological and Hydrological Institute
S-601 76 Norrköping, Sweden. Tel. +4611158000. Telex 644 00 smhi s.

ISSN 0347-2116